Cage Occupancy of Hydrogen in Mixed Gas Hydrates

TAKAAKI TSUDA

MARCH 2012

Cage Occupancy of Hydrogen in Mixed Gas Hydrates

A dissertation submitted to
THE GRADUATE SCHOOL OF ENGINEERING SCIENCE
OSAKA UNIVERSITY
in partial fulfillment of the requirements for the degree of
DOCTOR OF PHILOSOPHY IN ENGINEERING

BY

TAKAAKI TSUDA

MARCH 2012

TABLE OF CONTENTS

LIST OF FIGURES

LIST OF TABLES

ABSTRACT

Gas hydrate is one of inclusion compounds formed by some “cages”. These cages are constructed by hydrogen-bonded water molecules, and guest species is enclathrated into the cavity of cages. There is no chemical bond between hydrogen and hydrate cages in hydrogen hydrates, this means that molecular state hydrogen is entrapped into hydrate cages. These advantages promote hydrogen hydrate to become a candidate for hydrogen storage and transport material toward the society sustained by hydrogen energy. The author focuses on the fundamental studies for the utilization of hydrogen hydrates. The principal purpose of this research is analyzing the dependence of guest molecules on hydrate structure and cage occupancy of hydrogen. These factors are important for not only industrial utilization of hydrate as hydrogen storage material, but also scientific investigation on cage occupancy of guest molecules.

Part A involves two chapters and describes traditional type of clathrate hydrates, in particular structure-II hydrate systems. First of all, hydrogen + argon mixed-gas hydrate is studied by Raman spectroscopic analyses under three-phase (hydrate + water + fluid) conditions and at 77 K. Argon is enclathrated into both 5^{12} and $5^{12}6^4$ cages. In the equilibrium pressure region higher than approximately 25 MPa, four hydrogen cluster and argon competitively occupied $5^{12}6^4$ cages. In addition, Raman spectroscopic analysis at 77 K supports that the clusters of two, three, or four hydrogen molecules occupy $5^{12}6^4$ cages. Secondly, hydrogen + tetrahydrothiophene, furan, and cyclopentane mixed hydrates are studied by four-phase (hydrate + water + second component + gas) equilibrium and *p-V-T* measurements. All of these second components are non-hydrosoluble and enclathrated only into $5^{12}6^4$ cages, while all 5^{12} cages remain vacant. Hydrogen absorption rates of these hydrates are larger than that of tetrahydrofuran hydrate while their equilibrium storage amounts of hydrogen are comparable. Conversely, hydrogen storage abilities (rate, amount, and equilibrium temperature) of these hydrate are comparable with one another. In addition, The storage amounts of hydrogen would reach to about 1.0 mass% asymptotically at ~80 MPa.

In part B which contains four chapters, the author states some semi-clathrate hydrate systems. Hydrogen + tetra-*n*-butyl ammonium bromide, tetra-*n*-butyl ammonium fluoride, trimethylamine, and tetra-*n*-butyl phosphonium bromide are studied by phase equilibrium measurement and Raman spectroscopic analyses. These second components form semi-clathrate hydrates, which are different a little bit from ordinary clathrate hydrate, and are entrapped into large cages. On the other hand, hydrogen molecule occupies only small cage compartmentally. In hydrogen + the former two second components mixed hydrates, the structural transitions occur in accordance with the composition of solution and surrounding hydrogen fugacity. The occupied amount of hydrogen in the semi-clathrate hydrate significantly increases associated with the structural transition.

GENERAL INTRODUCTION

A. Gas Hydrate

1) Clathrate Hydrate [1]

Gas hydrate is one of the inclusion compounds, which is constructed by some "cages", and it is stabilized by entrapping the relatively small (guest) molecule into the cavity of cage. These cages are composed of hydrogen-bonded water molecules. In this thesis, gas hydrates are classified by how the guest molecules are enclathrated, one is clathrate hydrate, and the other is semi-clathrate hydrate. In clathrate hydrate, there is no chemical bond, but only van der Waals's force between the host water molecule and guest species. Typical cages are shown in **Fig. 1** and summarized in **Table 1** [1]. Oxygen atoms locate at all vertices of each face, and hydrogen atoms exist between oxygen atoms. According to the size of cavity, they are named as S-cage, S'-cage, M-cage, L-cage, and U-cage, respectively. In the type of cages, X^Y, X indicates type of faces (*e. g.*, "5" is pentagon), and Y represents the number of X in a cage.

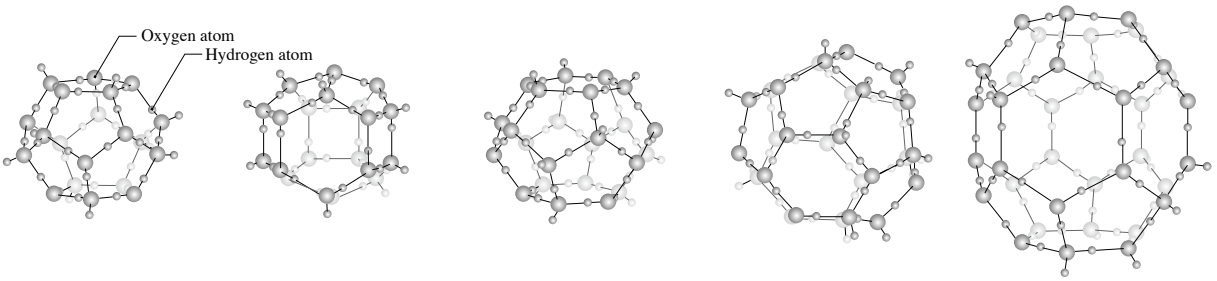

S-cage [5^{12}] S'-cage[$4^3 5^6 6^3$] M-cage [$5^{12}6^2$] L-cage [$5^{12}6^4$] U-cage [$5^{12}6^8$]

Fig. 1 Schematic illustration of hydrate cages constructing unit-cell structures.

Table 1 Summary on hydrate cages [1].

tag of cages	S-cage	S'-cage	M-cage	L-cage	U-cage
type of cages	5^{12}	$4^3 5^6 6^3$	$5^{12}6^2$	$5^{12}6^4$	$5^{12}6^8$
coordination number	20	20	24	28	36

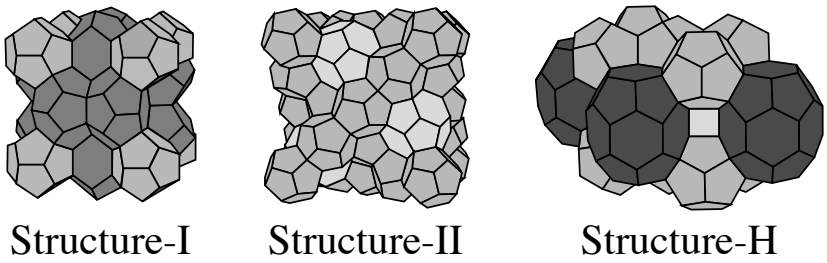

Fig. 2 Schematic illustration of hydrate unit-cell structures.

Table 2 Summary on unit-cells of clathrate hydrates [1].

type of unit-cell	**structure-I**		**structure-II**		**structure-H**		
kind of cages	S	M	S	L	S	S'	U
number of cages	2	6	16	8	3	2	1
diameter of free cavities / nm*	0.51	0.59	0.50	0.67	0.49**	0.51**	0.86**
H_2O per unit-cell	46		136		34		
crystal type	cubic		cubic		hexagonal		
space group	Pm3n		Fd3m		P6/mmm		
lattice constant *a*/nm	1.20		1.73		1.22		
lattice constant *c*/nm	-		-		1.01		

* The cavity diameter is obtained from the cavity radius minus the diameter of water (0.28 nm).

** From the atomic coordinates measured using single crystal X-ray diffraction on 2,2-dimethylpentane·5(Xe, H_2S)·34H_2O at 173 K [2].

These cages compose unit-cell structures in the fixed ratio. Typical unit-cell structures of clathrate hydrates are shown in **Fig. 2** and summarized in **Table 2** [1]. The diameter of free cavities and lattice constants are functions of temperature, pressure, and guest composition, that is, the values given are typical average values. In general, structure and stability of clathrate hydrates depend on size, shape, and physical property of guest species, additionally, temperature, pressure, and composition. Moreover, the closer the size between guest molecule and cavity size of hydrate cage, the more stable the hydrate lattice structure is (**Fig. 3**). Characteristics of each structure are briefly explained below;

• structure-I (s-I) hydrate

s-I hydrate is formed by relatively small guest molecule including hydrocarbon which has small carbon number (C1-C3). There is no direct face sharing between the S-cages. The structure can be constructed from the vertices of face-sharing M-cages arranged in columns with the M-cage sharing their opposing hexagonal faces.

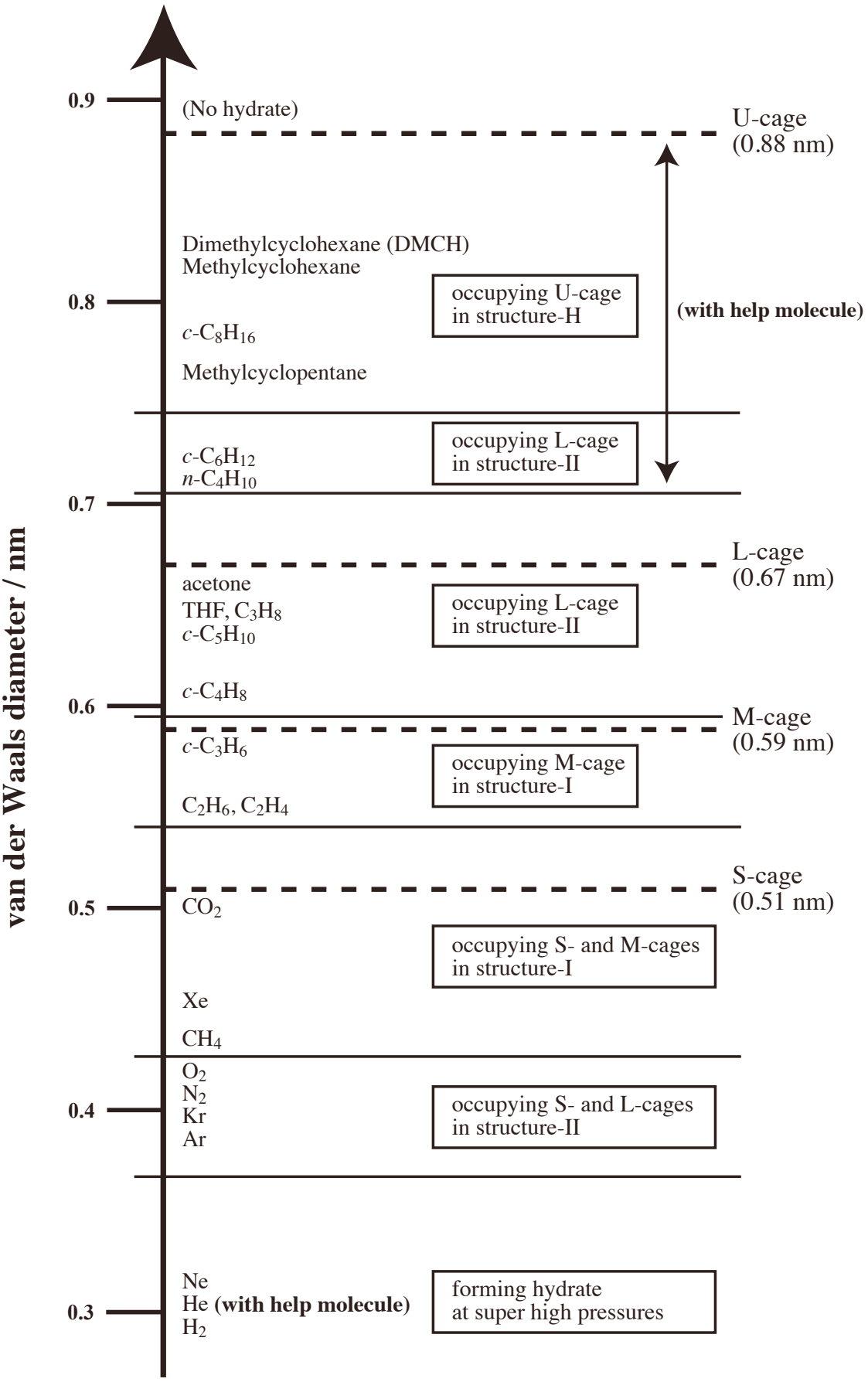

Fig. 3 Molecular diameter dependence on hydrate structures and cage occupancies [1, 3].

• structure-II (s-II) hydrate

s-II hydrate is formed by relatively large guest molecule including hydrocarbon which has slightly large carbon number (C3-C6), or drastically small molecule. The structure is built up of the layer of S-cages alternating with the layer of S-cages and L-cages, that is, S-cages are 3D-connected with one another.

• structure-H (s-H) hydrate

s-H hydrate is built up of the layer of S-cages with the layer of S'-cages and U-cages. In the case of s-H hydrates, a certain amount of small cages must be occupied by small guest molecules.

2) Semi-clathrate Hydrate [4]

Semi-clathrate hydrate is also one of gas hydrates, but different a little bit from ordinary clathrate hydrate. In the case of clathrate hydrate, all guest molecules are entrapped in each cage strictly. On the other hand, relatively large guest molecules such as amines involving tetraalkyl ammonium salts or tetraalkyl phosphonium salts form semi-clathrate hydrate. In this hydrate, nitrogen or phosphorous atom forms the frameworks of hydrogen bonds with water molecules, and residual alkyl groups lay astride several large cages where hydrogen bonds are partially broken, as small cages remain empty. Generally, one semi-clathrate hydrate has a number of unit-cell structures and cage occupancy of guest species. The feature of two well-known semi-clathrate hydrates, tetra-*n*-butyl ammonium bromide (hereafter, TBAB) and tetra-*n*-butyl ammonium fluoride (hereafter, TBAF) are summarized in **Table 3**, and a new cage, which named as L'-cage ($5^{12}6^3$) is introduced and shown in **Fig. 4** [4-6].

Table 3 Summary on the unit-cells of TBAB and TBAF semi-clathrate hydrates [4-8].

	TBAB hydrate						**TBAF hydrate**				
type of unit-cell	**TS-I (Type A)**			**RS (Type B)**			**CSS-I**		**TS-I**		
kind of cages	S	M	L'	S	M	L'	S	M	S	M	L'
number of cages	10	16	4	6	4	4	16	48	10	16	4
H_2O per unit-cell	624			76			343.2		164		
crystal type	tetragonal			orthorhombic			cubic		tetragonal		
TBA salts per unit-cell	24			2			12		5		
lattice constant *a*/nm	2.39			2.11			2.44		2.35		
lattice constant *b*/nm	-			1.26			-		-		
lattice constant *c*/nm	5.08			1.20			-		1.23		

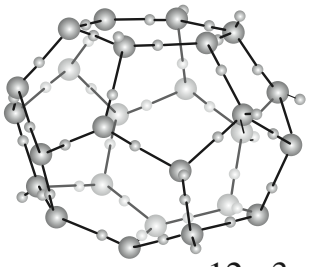

L'-cage [$5^{12}6^3$]

Fig. 4 Schematic illustration of L'-cage.

Various tetraalkyl ammonium or phosphonium salts ($X_4Y^+Z^-$; X = butyl or *iso*-amyl, Y = N or P, and Z = F, Cl, or Br) form semi-clathrate hydrate, while a large part of their unit-cell structures are still unclear [4].

B. Hydrogen Hydrate

1) Simple Hydrogen Hydrate

It had been considered that hydrogen (H_2) hydrate can not be formed, because H_2 molecule is too small to stabilize hydrate structures. In 1999, Dyadin *et al*. reported the phase diagram of H_2+H_2O mixed system shown in **Fig. 5**, and proved that H_2 hydrate existed in particular *p-T* conditions (100-360 MPa at the vicinity of 273 K) [9]. The diameter of H_2 molecule is so small that H_2 can form interstitial solid-solutions (filled-ice). As shown in **Fig. 5**, the filled-ice Ih is generated in the pressure region up to 100 MPa (displayed as "α"), while the filled-ice II is generated in the pressure region above 360 MPa (displayed as "β"). The simple H_2 hydrate is generated at pressures between the stable regions of two filled-ices, and it belongs to s-II unit-cell (displayed as "H").

The cage occupancy of H_2 in simple H_2 hydrate was firstly published by Mao *et al*. in 2002 [10]. They analyzed by means of XRD, and concluded that S-cage and L-cage were occupied by two and four H_2 clusters, respectively. After that, however, Lokshin *et al*. examined for D_2 deuterate, which means D_2 hydrate prepared from D_2+D_2O, by means of neutron diffraction, and reasoned that L-cage contained four D_2 clusters, while S-cage included only one D_2 molecule in itself [11].

Then, the S-cage occupancy of H_2 has been discussed and researched by means of various techniques, and they are inconsistent [12-15]. Although the occupancy might depend on sample preparation conditions, "single occupancy" is commonly supported.

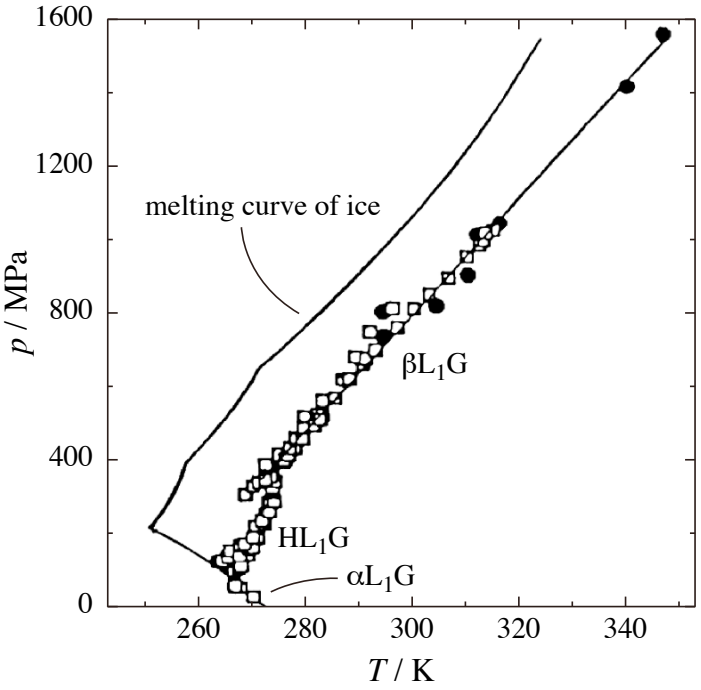

Fig. 5 Phase equilibrium (*p*-*T*) relation for H_2+H_2O mixed system [9].

2) Hydrogen + Second Component Mixed Hydrate

Assuming the single occupancy of H_2 in S-cages and quadruple occupancy in L-cages for simple H_2 hydrate, the maximum storage amount is ~3.8 mass%. As mentioned at section A, there is no chemical bond between H_2 and hydrate cages, this means that molecular state H_2 is entrapped into hydrate cages. These advantages promote H_2 hydrate to become a candidate for H_2 storage material toward the society sustained by H_2 energy (in detail about H_2 energy and its utility, see section C). On the other hand, there is a disadvantage of extra high pressure to stabilize simple H_2 hydrate.

Tetrahydrofuran (hereafter, THF) is an s-II hydrate former under atmospheric pressure, and all L-cages are occupied by THF molecules while all S-cages remain vacant. The addition of THF is able to reduce the equilibrium pressure of various simple hydrates, such as CH_4 and N_2 hydrates. In 2004, Florusse *et al*. firstly discovered that one H_2 molecule can be entrapped into each S-cage in H_2 + deuterated THF (THF-d_8) mixed deuterate, while all L-cages are occupied by THF-d_8 molecules at low pressures [16]. In this paper, the cage occupancy is decided by means of ^{1}H MAS NMR and volumetric measurements as 0.5 and 1.0, respectively. This discrepancy is due to a loss of H_2 during NMR. Finally, they conclude that some S-cages may be doubly occupied, whereas other ones are singly occupied based on the NMR line width of H_2. The theoretical maximum value of H_2 storage amount assuming the full occupancy of single H_2 in S-cages is ~1.0 mass%.

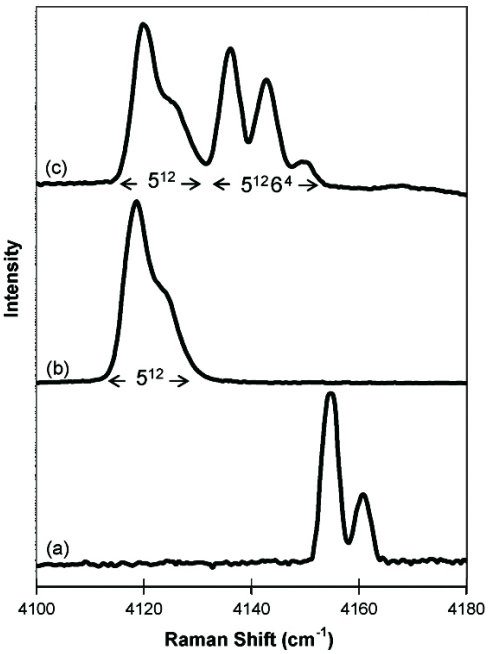

Fig. 6 Raman spectra obtained from (a) fluid, (b) H_2+THF mixed hydrate, and (c) simple H_2 hydrate phase [17].

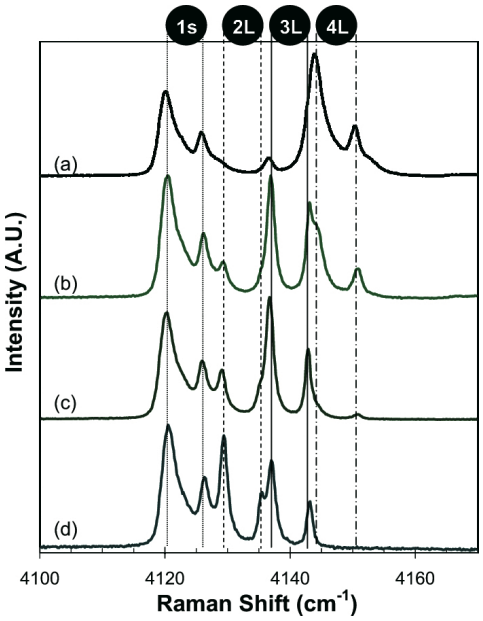

Fig. 7 Raman spectra obtained from simple H_2 hydrate phase at 76 K and 0.1 MPa [18].
(a): unperturbed hydrate,
(b)-(d): heat (150 K)/quench (76 K) cycles.

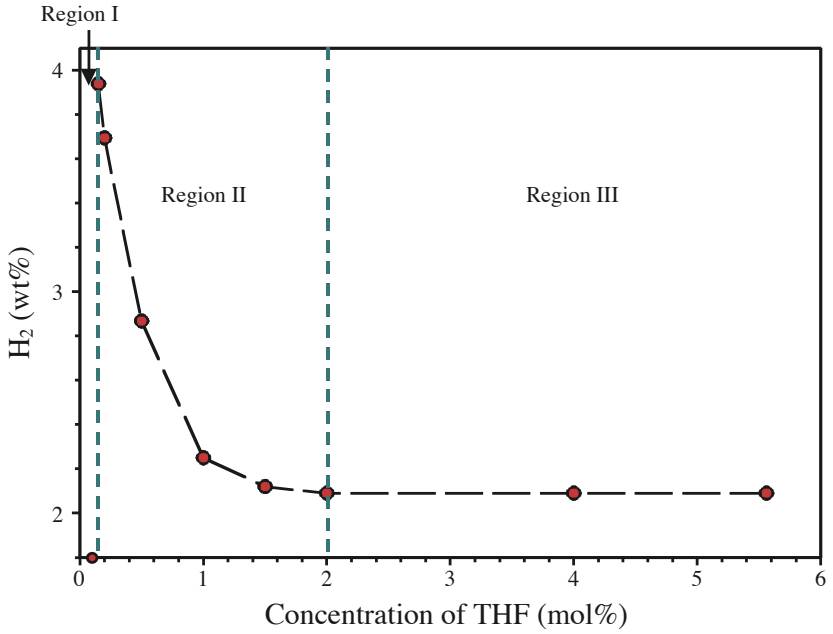

Fig. 8 H_2 content as a function of THF concentration [19].

Strobel *et al*. compared the Raman spectra obtained from simple H_2 hydrate and H_2+THF mixed hydrate, and decided that S-cages are singly occupied by H_2 molecule (**Fig. 6**, [17]). After that, the same group reported that S-cages and L-cages entrapped one and two, three, or four H_2 molecules,

respectively, in simple H_2 hydrate (**Fig. 7**, [18]). They labelled the Raman peaks obtained around ~4130 cm^{-1} as single H_2 occupied in S-cage, and double, triple, and quadruple H_2 in L-cage, in order of wave number. There are eight peaks, because each occupancy state has ortho- and para-H_2. Ortho means parallel nuclear spins, and para-H_2 has nuclear spin pair.

In addition, Lee *et al*. [19] and Sugahara *et al*. [20] reported that the increasing L-cage occupancy of H_2 attributed to the reducing that of THF, which is called "tuning effect" (shown in **Figs. 8-10**), measured by means of NMR and Raman spectroscopic analyses, respectively. They claimed the maximum H_2 storage values are ~4.0 mass% and ~3.4 mass%, respectively, where the discrepancy is due to the difference of occupancy in S-cage (2 H_2 *vs* 1 H_2).

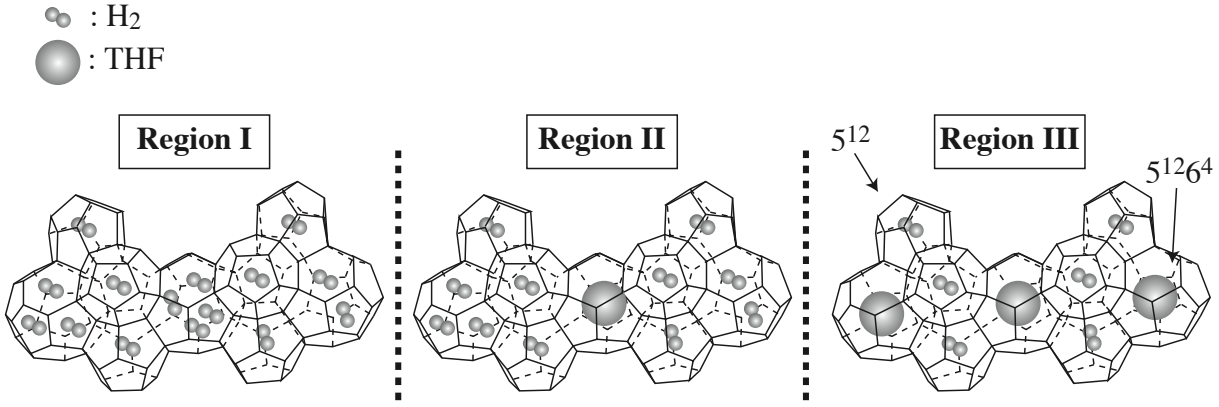

Fig. 9 Schematic diagram of H_2 distribution in the H_2+THF mixed hydrate [19].

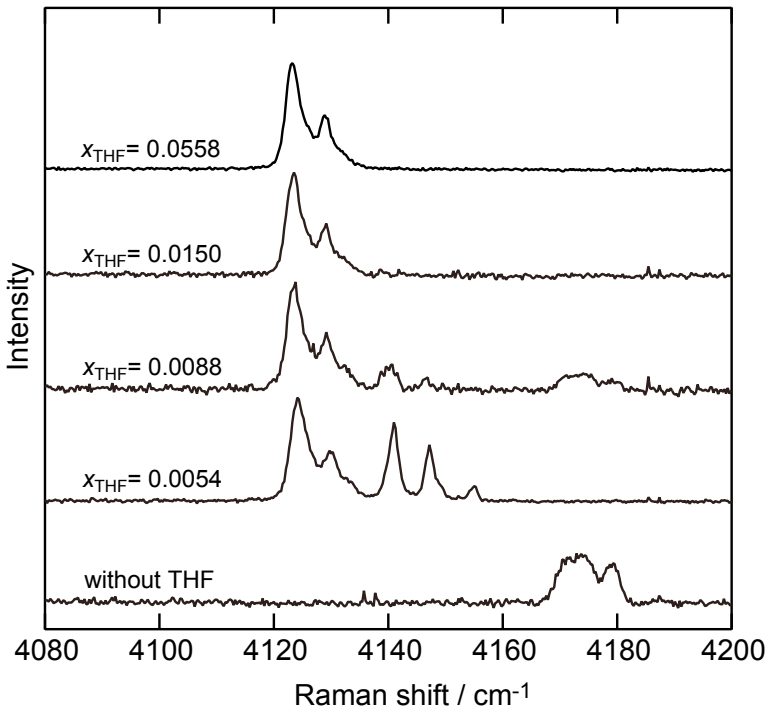

Fig. 10 Raman spectra corresponding to the H_2 vibrons in the H_2+THF mixed hydrates [20].

C. Sustainable Technology

1) Hydrogen Energy

In these days, there are a lot of issues accompanying the advance of science and technology. One of the severest issues is the environmental issue such as atmospheric pollution and global warming. This is attributable to the use of vast amounts of fossil fuel for the industry, the thermal power generation, and the traffic, etc. In order to overcome these problems, some ideas are provided. In the electrical production, for example, nuclear power generation is popular method in the US, France, and Japan, because it emits no CO_2, NO_x, and SO_x, and the cost of power generation is relatively low compared with other way. By contrast, there are always unusual risks of nuclear and radiation accidents. After "the Fukushima Daiichi nuclear disaster" following the Great East Japan Earthquake in March 2011, the world opinion is moving toward denuclearization.

Complying this trend, the comprehensively-clean energy sources and utility systems have been highly demanded. For example, wind energy, water energy, and solar energy are easily available, but utilizing these energy sources are limited by climate conditions. That is, intermittent and steady energy supply is slightly difficult. Hence, H_2 energy has attract much attention as a substitution, because of the advantages shown below;

(1) A large part of combustion product is H_2O

Similar to nuclear power, H_2 is zero emission material through its consumption.

(2) Feedstock to produce H_2 exists in diverse form and with a wide distribution

H_2 does not yield naturally, but is generated from fossil fuel by gas reforming, water by electrolyzation or photocatalysis, etc.

(3) Fuel cell (FC) has high generating-efficiency

FC converts chemical energy directly to electrical energy, and thermal energy generated simultaneously is able to be utilized. Thus, it has high generating-efficiency and integrated-efficiency (electrical energy + thermal energy).

Especially in point of **(2)**, the amount of water, which exists on the earth accounts for ~70 % of land surface, thus, there is ideal energy path (the endless cycle; primary energy source, translation, storage and transportation, and utilization) from water to water mediating H_2 as an energy carrier (shown in **Fig. 11**).

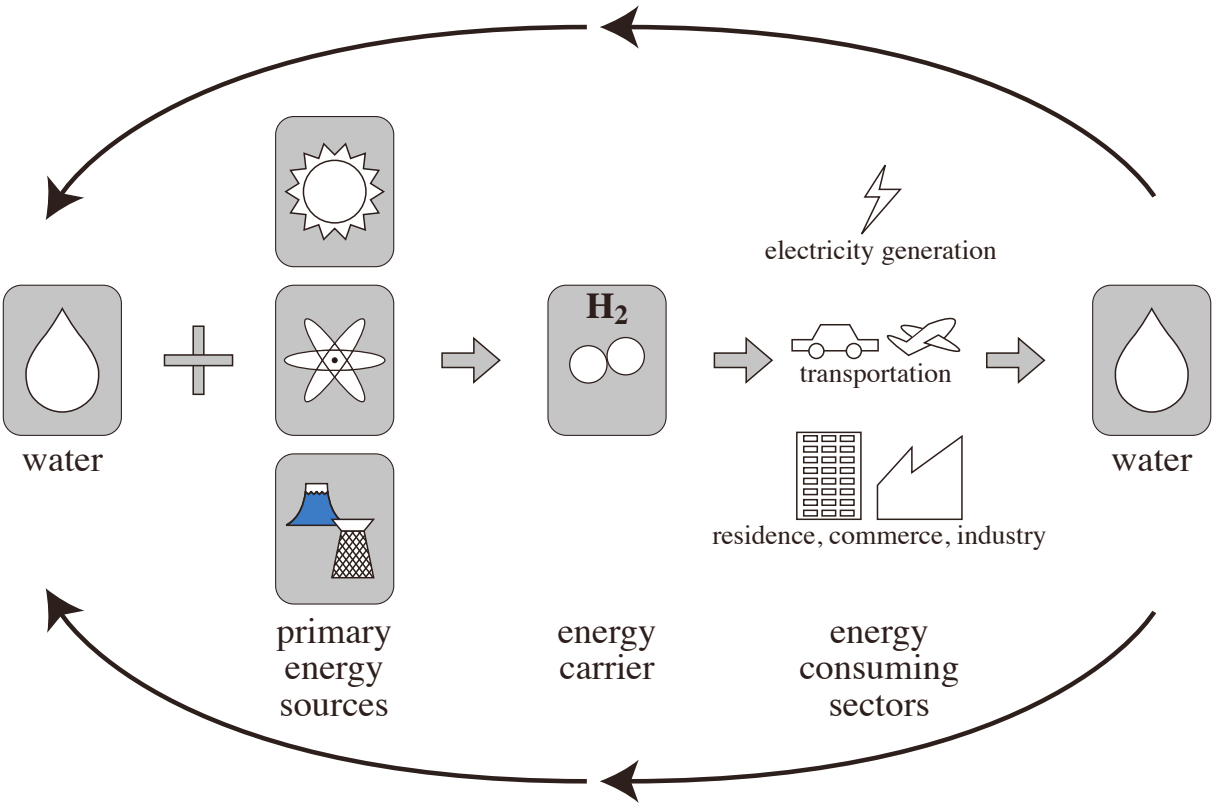

Fig. 11 H_2 energy cycle based on H_2 synthesized from water.

2) Utilizing Hydrogen [21, 22]

As mentioned above, H_2 energy is a possible breakthrough for energy and environmental issues. Currently, it does not yet become widespread, due to the many problems to be solved for utilizing. They are 1) production and supply, 2) separation and purification, and 3) storage and transportation. In this thesis, the author focuses especially on storage and transportation of H_2, and major methods are introduced.

Energy density per unit volume of H_2 is very low at standard temperature and pressure, hence developing highly-dense storage technique and material is desired as soon as possible. Common H_2 storage methods and their abilities are summarized in **Table 4**. The required conditions for H_2 storage materials are shown below;

(1) A large amount of H_2 storage

For FC vehicle use, storage amont of H_2 in a material is desired to be more than 5-6 mass%.

(2) Appropriate reaction time

Under the practical condition (>0.1 MPa, <420 K), the adequate H_2 storage and release rate is needed.

(3) Appropriate endurance

After 1000 storage and release cycles, it must remain more than 90 % of storage abilities.

Table 4 Common H_2 storage method.

method	storage ability	negative point
compressed H_2 tank (35 MPa and 70 MPa)	~3.5 mass%	hydrogen brittleness, cost and mass of tank
liquefied H_2 tank	~5 mass%	enormous energy for liquefying, boil off
chemical hydride	~3 mass%	high heat for endothermic dehydrogenating
MOF-5, MOF-177	~5 mass%	storage ability decreases drastically with temperature raising from 77 K

Furthermore, there are many problems to be solved, and there is no method that fulfill the all conditions of size, cost, safety, efficiency, conditions (pressure and temperature), and weight simultaneously. The innovative improvement and development are necessary immediately.

D. Research Purpose

As mentioned above, cage occupancy of guest molecules is easily-changed in accordance with kinds of second components and/or sample preparation methods and conditions. Thus, the principal purpose of this research is analyzing the dependence of guest molecules on hydrate structure and cage occupancy of H_2. These factors are important for not only industrial utilization of hydrate as H_2 storage material, but also scientific investigation on cage occupancy of guest molecules.

This thesis is divided into two parts, which are classified into six chapters according to the hydrate structure and cage occupancy of second component. Part A involves two chapters and describes traditional type of clathrate hydrates, in particular s-II hydrate systems. In Chapter 1, H_2 + argon mixed-gas hydrate is studied by Raman spectroscopic analyses under three-phase (hydrate + water + fluid) conditions and at 77 K. Argon is enclathrated into S- and L-cages of s-II hydrate. In Chapter 2, H_2 + tetrahydrothiophene, H_2 + furan, and H_2 + cyclopentane mixed hydrates are studied by phase equilibrium and *p-V-T* measurements. These second components are enclathrated into only L-cages of s-II hydrate. Part B contains four chapters and states some semi-clathrate hydrate systems. In Chapters 3-6, H_2+TBAB, H_2+TBAF, H_2 + trimethylamine, and H_2 + tetra-*n*-butyl phosphonium bromide are studied, respectively, by phase equilibrium measurement and Raman spectroscopic analyses. These second components are entrapped into large cages of semi-clathrate hydrate.

References

[1] Sloan, E. D.; Koh, C. A. "CLATHRATE HYDRATE OF NATURAL GASES, *Third Edition*.", CRC Press (2008).

[2] Udachin,K. A.; Ratcliffe, C. I.; Enright, G. D.; Ripmeester, J. A. "Structure H Hydrate: a Single Crystal Diffraction Study of 2,2-dimethylpentane·5(Xe, H_2S)·34H_2O.", *Supramolecular Chemistry*, **8(3)**, 173-176 (1997).

[3] Ripmeester, J. A.; Ratcliffe, C. I. "^{129}Xe NMR Studies of Clathrate Hydrates: New Guests for Structure II and Structure H.", *Journal of Physical Chemistry*, **94**, 8773-8776 (1990).

[4] Aladko, L. S.; Dyadin, Y. A.; Rodionova, T. V.; Terekhova, I. S. "Clathrate Hydrates of Tetrabutylammonium and Tetraisoamylammonium Halides.", *Journal of Structural Chemistry*, **43(6)**, 990-994 (2002).

[5] McMullan, R. K.; Bonamico, M.; Jeffrey, G. A. "Polyhedral Clathrate Hydrates. V. Structure of the Tetra-*n*-butyl Ammonium Fluoride Hydrate.", *Journal of Chemical Physics*, **39(12)**, 3295-3310 (1963).

[6] Shimada, W.; Shiro, M.; Kondo, H.; Takeya, S.; Oyama, H.; Ebinuma, T.; Narita, H. "Tetra-*n*-butylammonium Bromide-Water (1/38).", *Acta Crystallographica Section C*, **C61**, o65-o66 (2005).

[7] Shimada, W.; Ebinuma, T.; Oyama, H.; Kamata, Y.; Narita, H. "Free-growth Forms and Growth Kinetics of Tetra-*n*-butyl Ammonium Bromide Semi-clathrate Hydrate Crystals.", *Journal of Crystal Growth*, **274**, 246-250 (2005).

[8] Komarov, V. Y.; Radionova, T. V.; Terekhova, I. S.; Kuratieva, N. V. "The Cubic Superstructure-I of Tetra Butyl Ammonium Fluoride $(C_4H_9)_4NF29.7H_2O$ Clathrate Hydrate.", *Journal of Inclusion Phenomena and Macro cyclic Chemistry*, **59**, 11-15 (2007).

[9] Dyadin, Y. A.; Larionov, E. G.; Aladko, E. Y.; Manakov, A. Y.; Zhurko, F. V.; Mikina, T. V.; Komarov, V. Y.; Grachev, E. V. "Clathrate Formation in Water-Noble Gas (Hydrogen) Systems at High Pressures.", *Journal of Structural Chemistry*, **40**, 790-795 (1999).

[10] Mao, W. L.; Mao, H.; Goncharov, A. F.; Struzhkin, V. V.; Guo, Q.; Hu, J.; Shu, J.; Hemley, R. J.; Somayazulu M.; Zhao, Y. "Hydrogen Clusters in Clathrate Hydrate.", *Science*, **297**, 2247-2249 (2002).

[11] Lokshin, K. A.; Zhao, Y.; He, D.; Mao, W. L.; Mao, H. -K.; Hemley, R. J.; Lobanov, M. V.; Greenblatt, M. "Structure and Dynamics of Hydrogen Molecules in the Novel Clathrate Hydrate by High Pressure Neutron Diffraction.", *Physical Review Letters*, **93**, 125503-1-125503-4 (2004).

[12] Hashimoto, S.; Murayama, S.; Sugahara, T.; Sato, H.; Ohgaki, K. "Thermodynamic and Raman Spectroscopic Studies on H_2 + Tetrahydrofuran + Water and H_2 + Tetra-*n*-butyl Ammonium Bromide + Water Mixtures Containing Gas Hydrates.", *Chemical Engineering Science*, **61**, 7884-7888 (2006).

[13] Strobel, T. A.; Taylor, C. J.; Hester, K. C.; Dec, S. F.; Koh, C. A.; Miller, K. T.; Sloan, E. D., Jr. "Molecular Hydrogen Storage in Binary THF-H_2 Clathrate Hydrates.", *Journal of Physical Chemistry B*, **110**, 17121-17125 (2006).

[14] Wang, J.; Lu, H.; Ripmeester, J. A. "Raman Spectroscopy and Cage Occupancy of Hydrogen Clathrate Hydrate from First-Principle Calculations.", *Journal of American Chemical Society*, **131(40)**, 14132-14133, (2009).

[15] Chattaraj, P. K.; Bandaru, S.; Mondal, S. "Hydrogen Storage in Clathrate Hydrates.", *Journal of Physics and Chemistry A*, **115**, 187-193 (2011).

[16] Florusse, L. J.; Peters, C. J.; Schoonman, J.; Hester, K. C.; Koh, C. A.; Dec, S. F.; Marsh K. N.; Sloan, E. D. "Stable Low-Pressure Hydrogen Clusters Stored in a Binary Clathrate Hydrate.", *Science*, **306**, 469-471 (2004).

[17] Strobel, T. A.; Koh, C. A.; Sloan, E. D. "Hydrogen Storage Properties of Clathrate Hydrate Materials.", *Fluid Phase Equilibria*, **261**, 382-389 (2007).

[18] Strobel, T. A.; Sloan, E. D.; Koh, C. A. "Raman Spectroscopic Studies of Hydrogen Clathrate Hydrates.", *Journal of Chemical Physics*, **130**, 014506-1-014506-10 (2009).

[19] Lee, H.; Lee, J. -W.; Kim, D. Y.; Park, J.; Seo, Y. -T.; Zeng, H.; Moudrakovski, I. L.; Ratcliffe, C. I.; Ripmeester, J. A. "Tuning Clathrate Hydrates for Hydrogen Storage.", *Nature*, **434**, 743-746 (2005).

[20] Sugahara, T.; Haag, J. C.; Prasad, P. S. R.; Warntjes, A. A.; Sloan, E. D.; Sum, A. K.; Koh, C. A. "Increasing Hydrogen Storage Capacity Using Tetrahydrofuran.", *Journal of American Chemical Society*, **131(41)**, 14616-14617, (2009).

[21] Bysby, L. R. "Hydrogen and Fuel Cells (a comprehensive guide).", PennWell Corporation (2005).

[22] Styapal, S. “Hydrogen Program Overview.”, 2009 DOE Hydrogen Program and Vehicle Technologies Program, Annual Merit Review and Peer Evaluation Meeting, (2009).

Chapter 1

Competitive Cage Occupancy of Hydrogen and Argon in Structure-II Hydrates

Abstract

The cage occupancy of hydrogen in the single-crystals of simple hydrogen hydrates and hydrogen + argon mixed-gas hydrates was investigated by means of *in situ* Raman spectroscopy under the three-phase (hydrate + water + fluid) equilibrium condition. In the equilibrium pressure region higher than approximately 25 MPa, four hydrogen cluster and argon competitively occupied the large cages of structure-II hydrogen + argon mixed-gas hydrates. In addition, Raman spectroscopic analysis at 77 K supports that the clusters of two, three, or four hydrogen molecules occupy large cages.

Keywords: Gas hydrate, Hydrogen, Raman spectroscopy, Cage occupancy, High pressure

1. 1. Introduction

Hydrogen (H_2) occupancy in (H_2 + other guest species) mixed-gas hydrates is scientifically interesting and important. **Table 1-1** shows H_2 occupancy in the hydrate generated from various gas mixtures containing H_2. At the present time, there is no reference to the H_2 occupancy in the hydrate cages of the s-I CH_4 [1], C_2H_6 [2], and *c*-C_3H_6 [2] hydrates on the stability boundary of hydrates formed from H_2 and s-I formers. With the coexistence of C_3H_8 [2, 3] or tetrahydrofuran (hereafter, THF) [4-6] that occupies only the L-cage in s-II hydrate, H_2 occupies empty S-cage. In the H_2+THF mixed hydrates, the L-cage is partially occupied by H_2 under the specific condition [5]. Additionally, so far, there is no report on cage occupancies of H_2 in the s-II hydrate formed from H_2 with small guest species like argon (Ar).

In Chapter 1, simple H_2 hydrates and H_2+Ar mixed-gas hydrates are investigated. There have been some important reports on the hydrate cage occupancy of Ar and H_2; Ar and H_2 molecules occupy both S- and L-cages of each s-II simple gas hydrate [7, 8]. In addition, the both molecules are able to multiply occupy the L-cage [8-12]. To investigate competitive cage occupancy of such small guest species is interesting and significant from the viewpoint of the H_2 hydrate sciences. In the H_2+Ar mixed-gas hydrate system, the cage occupancies of H_2 under the three-phase (hydrate + water + fluid) equilibrium conditions were measured by means of *in situ* Raman spectroscopy at 276.1 K. Additionally, the H_2 occupancy in L-cage was evaluated from Raman peaks at 77 K.

1. 2. Experimental

1. 2. 1. Apparatus

The high-pressure optical cell for Raman spectroscopic analysis had a pair of highly pure sapphire windows (Ti free) on both the upper and lower sides. This high-pressure optical cell was the same as previous one [2] (shown in **Figs. 1-1, 1-2**). The temperature-controlled water was circulated in the exterior jacket of the high-pressure optical cell. A ruby ball was enclosed into the high-pressure optical cell. The contents were agitated by the ruby ball, which was rolled around by vibration from outside.

The system temperature was measured within an uncertainty of 0.02 K using a thermistor probe (Takara D-641), which was inserted into a hole in the cell wall. The system pressure was measured by a pressure gauge (NMB CSD-701B) with an estimated maximum uncertainty of 2 MPa.

Table 1-1 Hydrogen occupancy in the hydrate.

second component	cage occupancies of second components	H_2 occupancy	conditions
CH_4	s-I, S and M-cages	-	low-temperature [1]
C_2H_6, *c*-C_3H_6	s-I, M-cage	-	three-phase equilibrium [2]
C_3H_8	s-II, L-cage	S-cage	three-phase equilibrium [2]
		S-cage	low-temperature [3]
THF	s-II, L-cage	S-cage	three-phase equilibrium [4, 6]
		S- and L-cages	low-temperature [5]

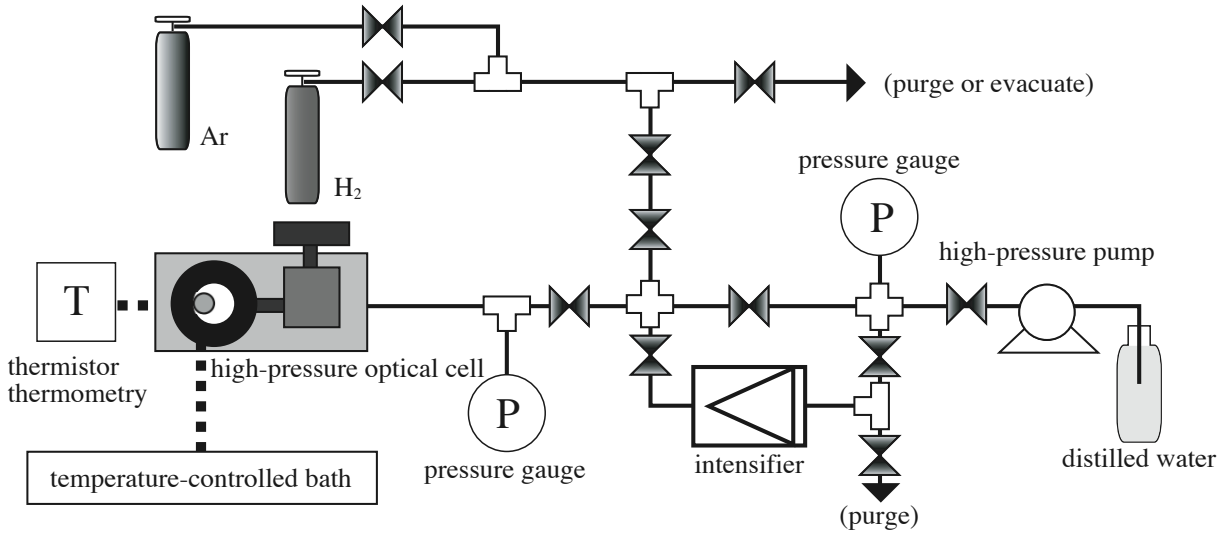

Fig. 1-1 Schematic illustration of experimental apparatus for Raman spectroscopic measurement.

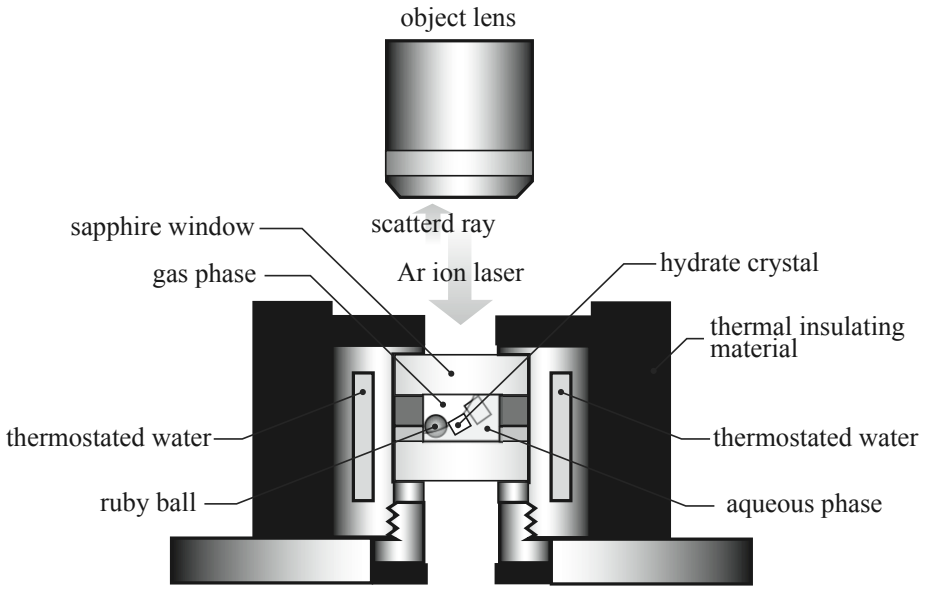

Fig. 1-2 Cross sectional view of high-pressure optical cell.

1. 2. 2. Procedures

The gas mixture of H_2 and Ar prepared at a specific concentration was introduced into the evacuated high-pressure optical cell, and the content was pressurized up to a desired pressure by supplying water. A lot of gas hydrates were primarily generated by efficient agitation, then the system temperature was gradually risen to leave a few seed crystals. Since then the system temperature was dropped little by little to prepare the single-crystal of the hydrate under the three-phase (hydrate + water + mixed fluid of H_2 and Ar) coexisting state. In this thesis, the single-crystal of hydrate was confirmed by the Raman spectra based on the O–O stretching vibration. The appearance of single-crystals could be observed by use of the CCD camera through the upper sapphire window. **Figure 1-3** shows a typical photo of single-crystals prepared from H_2+Ar mixed-gas hydrate system. Such hydrate crystals were analyzed through a sapphire window using a laser Raman microprobe spectrophotometer with multichannel CCD detector. The Ar-ion laser beam (wavelength: 514.5 nm, laser spot diameter: 2 μm) from the object lens was irradiated to the sample through the upper sapphire window. The backscatter was taken in with the same lens. The spectral resolution was about 0.7 cm^{-1}.

1. 2. 3. Materials

Research grade H_2 and Ar (both mole fraction purities: 0.999999) were obtained from Japan Air Gases Co., Ltd. The maximum impurity was 0.2 ppm of nitrogen. The distilled water was obtained from the Wako Pure Chemical Industries, Ltd. All of them were used without further purifications.

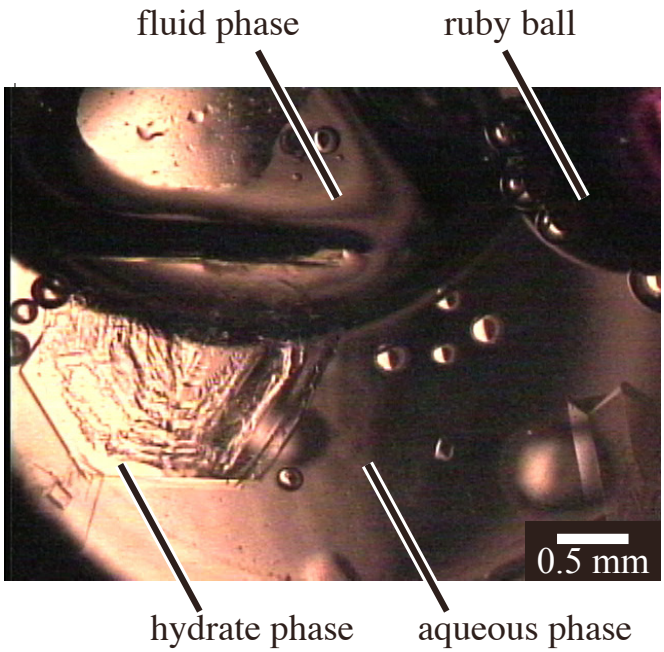

Fig. 1-3 Photo of single-crystals of H_2+Ar mixed-gas hydrate.

1. 3. Results and Discussion

Raman peaks corresponding to the intramolecular H–H stretching vibration modes of H_2 in L-cage are strongly affected by surrounding temperature [8]. However, there is no report on the Raman spectra of H_2 in simple H_2 hydrate at the vicinity of experimental temperature (~276 K) of present study. Therefore, first of all, Raman spectroscopic analyses have been performed in the single-crystal of simple H_2 hydrates to discuss H_2 occupancy in L-cage based on the comparison with the spectra of H_2+Ar mixed-gas hydrates. The Raman spectra obtained from the single-crystal of simple H_2 hydrate under the three-phase equilibrium conditions are shown in **Fig. 1-4**. The three peaks corresponding to the H–H vibration were detected at 4132, 4144, and 4152 cm^{-1} in the hydrate phase. These peaks are fitted by use of Voigt function with the baseline correction. Our previous study indicated that the Raman peak corresponding to H_2 in S-cage is detected at 4132 cm^{-1} at similar temperatures [13]. Hence, we can distinguish that the peaks corresponding to the H_2 molecules in L-cage are detected at 4144 and 4152 cm^{-1}. The peak intensity of 4152 cm^{-1} becomes large with increasing pressure.

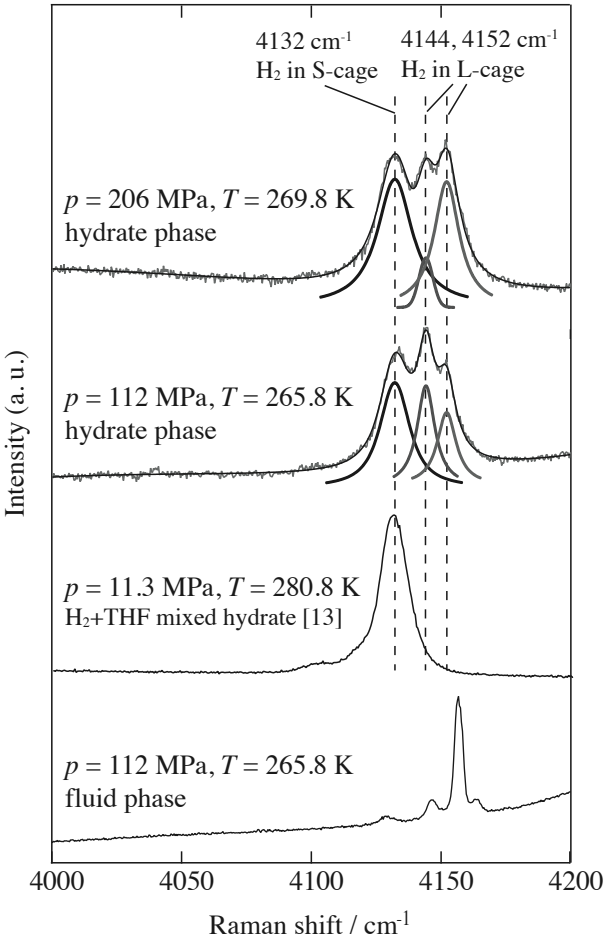

Fig. 1-4 Raman spectra corresponding to the H–H stretching vibration mode of H_2 for simple H_2 hydrate and H_2+THF mixed hydrate [13]. The thick solid line is fitted Voigt curves for each peak in the hydrate phase.

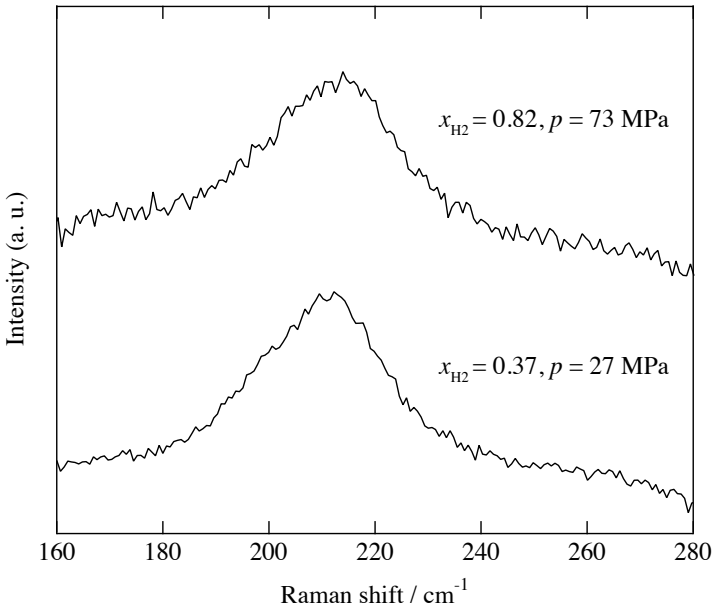

Fig. 1-5 Raman spectra corresponding to the O–O stretching vibration in the H_2+Ar mixed-gas hydrate system at 276.1 K.

The Raman spectra of the hydrate single-crystals prepared from H_2+Ar mixed-gas and water were measured under the three-phase equilibrium conditions at 276.1 K. The Raman spectra corresponding to the O–O stretching vibration in the hydrate crystals are shown in **Fig. 1-5**. In our previous study, it was reported that the pressure dependence of Raman peak corresponding to O–O stretching vibration mode along the stability boundary of hydrate is peculiar to the unit lattice of hydrates [7, 14, 15]. The Raman peaks of the O–O stretching vibration of the H_2+Ar mixed-gas hydrates are detected at 210 cm^{-1} (27 MPa) and 212 cm^{-1} (73 MPa), which agree with those of other s-II hydrate systems [7, 14, 15]. Therefore, the s-II hydrate is generated from H_2+Ar+water ternary system in the pressure region of the present study.

The Raman spectra corresponding to the H–H stretching vibration in H_2+Ar mixed-gas hydrate system at 276.1 K are shown in **Fig. 1-6**. Each peak is fitted by use of Voigt function with the baseline correction. Multiple peaks of H_2 vibron were detected at 4132, 4143, and 4151 cm^{-1} in the hydrate phase at equilibrium pressures higher than ~25 MPa. The peak positions of H_2+Ar mixed-gas hydrates are similar to those of simple H_2 hydrate. That is, the peak detected at 4131 cm^{-1} is derived from H_2 in S-cage, and the peaks detected at 4143 and 4151 cm^{-1} correspond to the H_2 molecules in L-cage. Equilibrium pressures lower than simple H_2 hydrate clearly indicate that Ar is enclathrated in hydrate cages and H_2 molecule occupies both S- and L-cages competitively with Ar. Interestingly, the Raman peak (at 4151 cm^{-1}) of H_2 in 4 H_2 cluster was detected at a low pressure like 27 MPa as shown in **Fig. 1-6**. The peak detected at 4143 cm^{-1} obtained from H_2+Ar mixed-gas hydrates decays more than that of 4151 cm^{-1} with decreasing equilibrium pressure (H_2 concentration), while simple H_2 hydrate has a opposite trend. There are two possible interpretations of the trend. One is that the contribution of two

(or three) H_2 molecules to L-cage stabilization is weaker than that of Ar though four H_2 molecules are comparable to Ar. The other is simultaneous H_2 occupancy with Ar into L-cages.

To obtain advanced information on L-cage occupancy of H_2, Raman spectroscopic analyses were also performed for the H_2+Ar mixed-gas hydrate at 77 K. The sample of this experiment was prepared from finely ground ice (~375 μm) pressurized with H_2+Ar mixed-gas at 60.3 MPa and 253 K. The Raman spectrum corresponding to the H–H stretching vibration obtained at 77 K is shown in **Fig. 1-7**. Multiple peaks of H_2 vibron were detected at between 4120 and 4160 cm^{-1}. Based on the comparison with the peaks which are identified in simple H_2 hydrate system [16], these peaks can be separated into

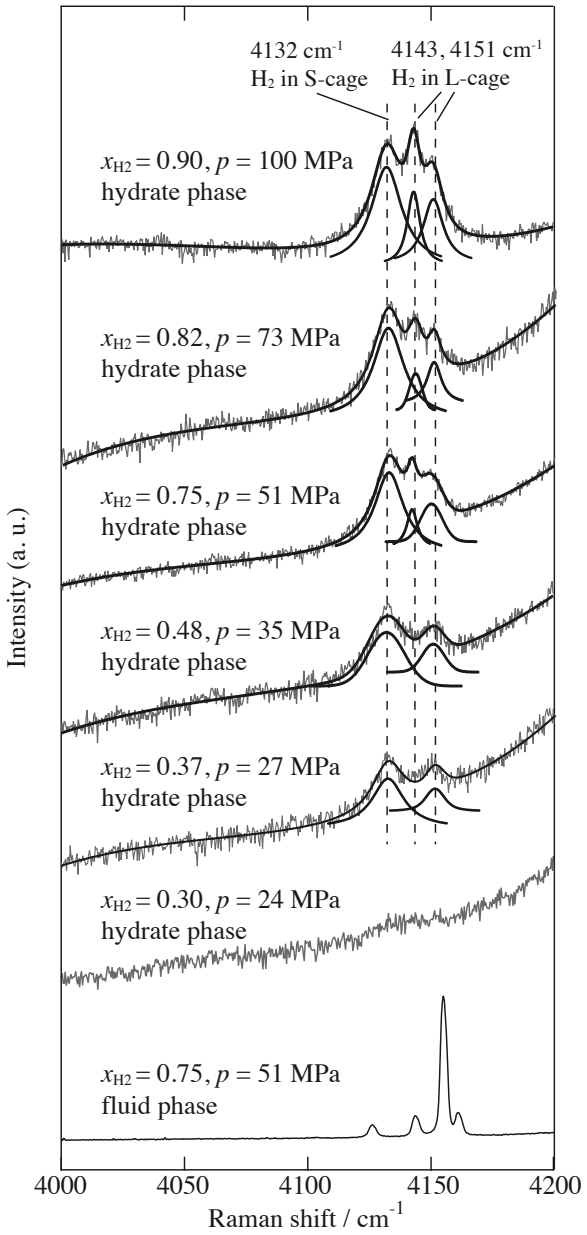

Fig. 1-6 Raman spectra corresponding to the H–H stretching vibration mode of H_2 in the H_2+Ar mixed-gas hydrate systems at 276.1 K. In the hydrate phase, the thick solid line is the Voigt curve fitted for each peak.

eight peaks corresponding to one ortho- (or para-) H_2 molecule in S-cage, and two, three, or four ortho- (or para-) H_2 molecules in the L-cage. This result reveals that L-cage in the H_2+Ar mixed-gas hydrate is occupied by a cluster of two, three, or four H_2 molecules similar as in the case with simple H_2 hydrate. Based on the reports on the multiple occupancy of H_2 [8, 9] and Ar [10-12] in the L-cage of the each simple hydrate, there is a possibility for the simultaneous H_2 occupancy with Ar in an L-cage of the s-II H_2+Ar mixed-gas hydrates. The possibility of simultaneous L-cage occupancy of two different molecules in s-II THF+He mixed hydrates was also reported [17]. Taken into consideration the concept of entropy, heterogeneous clusters of H_2 and Ar should occupy L-cages because the void space of L-cage is large enough. However, the peak shift attributed to the simultaneous L-cage occupancy of H_2 and Ar was not observed. If H_2 and Ar simultaneously occupy a L-cage, the additional Raman peaks of H_2 in the L-cage would be overlapped with other peaks. Further investigation by other experimental method such as neutron diffraction is needed to make clear simultaneous H_2 occupancy with Ar in an L-cage.

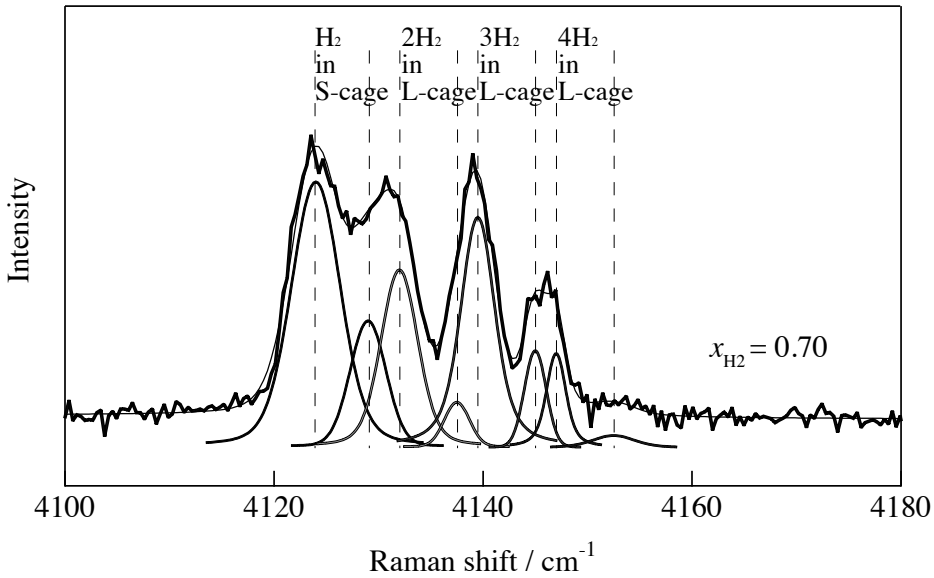

Fig. 1-7 Raman spectrum corresponding to the H–H stretching vibration mode of H_2 for H_2+Ar mixed-gas hydrate at 60.3 MPa and 253 K. It was recorded at 0.1 MPa and 77 K.

1. 4. Conclusion

Raman spectroscopic analyses were performed at 276.1 K to investigate the H_2 occupancy in the simple H_2 hydrate and the H_2+Ar mixed-gas hydrate systems under the three-phase equilibrium conditions. Raman spectra reveal that the H_2+Ar mixed-gas hydrates form s-II lattice. One of the most important findings in the present study is that four H_2 clusters occupy the L-cages competitively with Ar in the equilibrium pressure region higher than ~25 MPa at an ambient temperature. In the H_2+Ar mixed-gas hydrates, the pressure dependence of L-cage occupancy of H_2 differs from that of simple H_2 hydrates. In addition, Raman spectroscopic analysis at 77 K reveals that the cluster of two, three, or four H_2 occupies the L-cage of the H_2+Ar mixed-gas hydrates.

Notation

p: pressure [Pa]
T: temperature [K]
x_{H2}: H_2 composition in the feed gas mixture [-]

References

[1] Skiba, S. S.; Larionov, E. G.; Manakov, A. Y.; Kolesov, B. A.; Kosyakov, V. I. "Investigation of Hydrate Formation in the System H_2-CH_4-H_2O at a Pressure up to 250 MPa.", *Journal of Physics and Chemistry B*, **111**, 11214-11220 (2007).

[2] Sugahara, T.; Mori, H.; Sakamoto, J.; Hashimoto, S.; Ogata, K.; Ohgaki, K. "Cage Occupancy of Hydrogen in Carbon Dioxide, Ethane, Cyclopropane, and Propane Hydrates.", *The Open Thermodynamics Journal*, **2**, 1-6 (2008).

[3] Skiba, S. S.; Larionov, E. G.; Manakov, A. Y.; Kolesov, B. A.; Ancharov, A. I.; Aladko, E. Y. "Double Clathrate Hydrate of Propane and Hydrogen.", *Journal of Inclusion Phenomena and Macrocyclic Chemistry*, **63**, 383-386 (2009).

[4] Florusse, L. J.; Peters, C. J.; Schoonman, J.; Hester, K. C.; Koh, C. A.; Dec, S. F.; Marsh K. N.; Sloan, E. D. "Stable Low-Pressure Hydrogen Clusters Stored in a Binary Clathrate Hydrate.", *Science*, **306**, 469-471 (2004).

[5] Lee, H.; Lee, J. -W.; Kim, D. Y.; Park, J.; Seo, Y. -T.; Zeng, H.; Moudrakovski, I. L.; Ratcliffe, C. I.; Ripmeester, J. A. "Tuning Clathrate Hydrates for Hydrogen Storage.", *Nature*, **434**, 743-746 (2005).

[6] Hashimoto, S.; Sugahara, T.; Sato, H.; Ohgaki, K. "Thermodynamic Stability of H_2 + Tetrahydrofuran Mixed Gas Hydrate in Nonstoichiometric Aqueous Solutions.", *Journal of Chemical & Engineering Data*, **52**, 517-520 (2007).

[7] Sugahara, K.; Kaneko, R.; Sasatani, A.; Sugahara, T.; Ohgaki, K. "Thermodynamic and Raman Spectroscopic Studies of Ar Hydrate System.", *The Open Thermodynamics Journal*, 2, 95-99 (2008).

[8] Mao, W. L.; Mao, H.; Goncharov, A. F.; Struzhkin, V. V.; Guo, Q.; Hu, J.; Shu, J.; Hemley, R. J.; Somayazulu M.; Zhao, Y. "Hydrogen Clusters in Clathrate Hydrate.", *Science*, **297**, 2247-2249 (2002).

[9] Lokshin, K. A.; Zhao, Y.; He, D.; Mao, W. L.; Mao, H. -K.; Hemley, R. J.; Lobanov, M. V.; Greenblatt, M. "Structure and Dynamics of Hydrogen Molecules in the Novel Clathrate Hydrate by High Pressure Neutron Diffraction.", *Physical Review Letters*, **93**, 125503-1-125503-4 (2004).

[10] Shimizu, H.; Hori, S.; Kume, T.; Sasaki, S. "Optical Microscopy and Raman Scattering of a Single Crystalline Argon Hydrate at High Pressures.", *Chemical Physics Letters*, **368**, 132-138 (2003).

[11] Tanaka, H.; Nakatsuka, T.; Koga, K. “On the Thermodynamic Stability of Clathrate Hydrates IV: Double Occupancy of Cages.”, *Journal of Chemical Physics*. **121**, 5488-5493 (2004).

[12] Manakov, A. Y.; Voronin, V. I.; Kurnosov, A. V.; Teplykh, A. E.; Komarov, V. Y.; Dyadin, Y. A. “Structural Investigations of Argon Hydrates at Pressure up to 10 kbar.”, *Journal of Inclusion Phenomena and Macrocyclic Chemistry*, 48, 11-18 (2004).

[13] Hashimoto, S.; Murayama, S.; Sugahara, T.; Sato, H.; Ohgaki, K. “Thermodynamic and Raman Spectroscopic Studies on H_2 + Tetrahydrofuran + Water and H_2 + Tetra-*n*-butyl Ammonium Bromide + Water Mixtures Containing Gas Hydrates.”, *Chemical Engineering Science*, **61**, 7884-7888 (2006).

[14] Sugahara, K.; Tanaka, Y.; Sugahara, T.; Ohgaki, K. “Thermodynamic Stability and Structure of Nitrogen Hydrate Crystal.”, *Journal of Supramolecular Chemistry*, **2**, 365-368 (2002).

[15] Sugahara, K.; Sugahara, T.; Ohgaki, K. “Thermodynamic and Raman Spectroscopic Studies of Xe and Kr Hydrates.”, *Journal of Chemical & Engineering Data*, **50**, 274-277 (2005).

[16] Strobel, T. A.; Sloan, E. D.; Koh, C. A. “Raman Spectroscopic Studies of Hydrogen Clathrate Hydrates.”, *Journal of Chemical Physics*, **130**, 014506-1-014506-10 (2009).

[17] Papadimitriou, N. I.; Tsimpanogiannis, I. N.; Stubos, A. K.; Martin, A.; Rovetto, L. J.; Peters, C. J. “Unexpected Behavior of Helium as Guest Gas in SII Binary Hydrates.”, *Journal of Physical Chemistry Letters*, **1**, 1014-1017 (2010).

Chapter 2

Effect of Additives on Small-cage Occupancy of Hydrogen in Structure-II Hydrates

Abstract

In this study, hydrogen absorption rate of structure-II clathrate hydrates was focused. Tetrahydrothiophene, furan, and cyclopentane was adopted as second components (additives), and then the cage occupancy of hydrogen was measured by *p-V-T* measurement. Hydrogen absorption rates of these hydrates are larger than that of tetrahydrofuran hydrate while their equilibrium storage amounts of hydrogen are comparable. Conversely, hydrogen storage abilities (rate, amount, and equilibrium temperature) of these hydrate are comparable with one another. In addition, The storage amounts of hydrogen would reach to about 1.0 mass% asymptotically at ~80 MPa.

Keywords: Gas hydrate, Phase equilibria, Stability, Cage occupancy, High pressure, Absorption

2. 1. Introduction

Highly efficient and safe storage and transport of H_2 under mild conditions are desired for realizing new world that demands on H_2 energy. As one of candidates, H_2 clathrate hydrates attract the attention, because they are able to store H_2 in molecular state and a large part of them is composed of H_2O, which means environmentally friendly. In particular, the H_2 mixed hydrates, which involve the secondary components (additives), have been attracted alternatively [1-5]. The additives would moderate the conditions of mixed hydrate formation drastically.

Tetrahydrofuran (hereafter, THF) is familiar as an additive, which forms s-II hydrate and occupies its L-cages. THF hydrate has empty sixteen S-cages and eight L-cages per unit lattice. The ratio of S-cages to all cages of hydrate unit-cell for s-II is the second largest of all hydrate structures. It is well known that the ratio for s-H hydrate is the largest, however, a small help molecule is essential to prepare s-H hydrates. Therefore, it is impossible to store and release H_2 through the additive hydrate without destruction of hydrate cages. Actually, there are a few reports about the reversible storage and release of H_2 by pressurizing or depressurizing without the destruction of hydrate cages for THF hydrates [6, 7]. Their results are coincident with one another on the point of maximum H_2 storage amount. The storage amount of H_2 reaches a plateau of increase {2.0 mol (H_2) / mol (THF hydrate)} in the vicinity of 80 MPa. Compared with H_2 storage in H_2 absorbing alloys, this technique is simple and low energy-loss for H_2 storage, because the heating to release H_2 is not necessary. Not only storage amount but also storage rate is one of the most important factors for the reversible storage and release of H_2.

In Chapter 2, tetrahydrothiophene (hereafter, THT), furan, and cyclopentane (*c*-C_5H_{10}) were adopted as additives for the H_2 storage using gas hydrates. These additives are similar in molecular size and shape to one another and THF, and enable us to evaluate what kind of effect the additives would have on H_2 storage abilities, for example, the presence or absence of double bond, the existence of hetero atom, and so on. Thermodynamic stability of H_2 + additive mixed systems and the H_2 storage amount and rate in these additive hydrates were investigated.

2. 2. Experimental

2. 2. 1. Apparatus

Two types of high-pressure cell were used for phase equilibrium measurements. Both of them are similar to the previous ones [3, 5] (shown in **Figs. 2-1, 2-2**). The high-pressure cell made of stainless steel had an inner volume of *ca*. 150 cm^3 [3]. The maximum working pressure was 10 MPa. The cell had a set of windows for visually observing the phase behavior. The other was pressure-proof glasscell [5]. The inner volume and maximum working pressure of the high-pressure glass cell were 10 cm^3 and 5 MPa, respectively. All parts of the high-pressure cell were immersed in a temperature-controlled water bath. The contents were agitated using an up-and-down mixing bar driven by an exterior permanent magnetic ring. The experimental apparatus for the *p-V-T* measurements is the same as the previous one [6] (shown in **Fig. 2-3**). The inner volume of a larger high-pressure cell (cell I) was 100 cm^3, and that of the smaller one (cell II) was 10 cm^3. The maximum working pressure of these high-pressure cells was 75 MPa. All parts of the cells were immersed in a temperature-controlled water bath. The system temperature was measured with in an uncertainty of 0.02 K using a thermistor probe (Takara D-632). The probe was calibrated with a Pt resistance thermometer defined by ITS-90. The system pressure was measured by a pressure gauge (Valcom VPRT) with an estimated maximum uncertainty of 0.01 MPa (<10 MPa) and 0.1 MPa (>10 MPa).

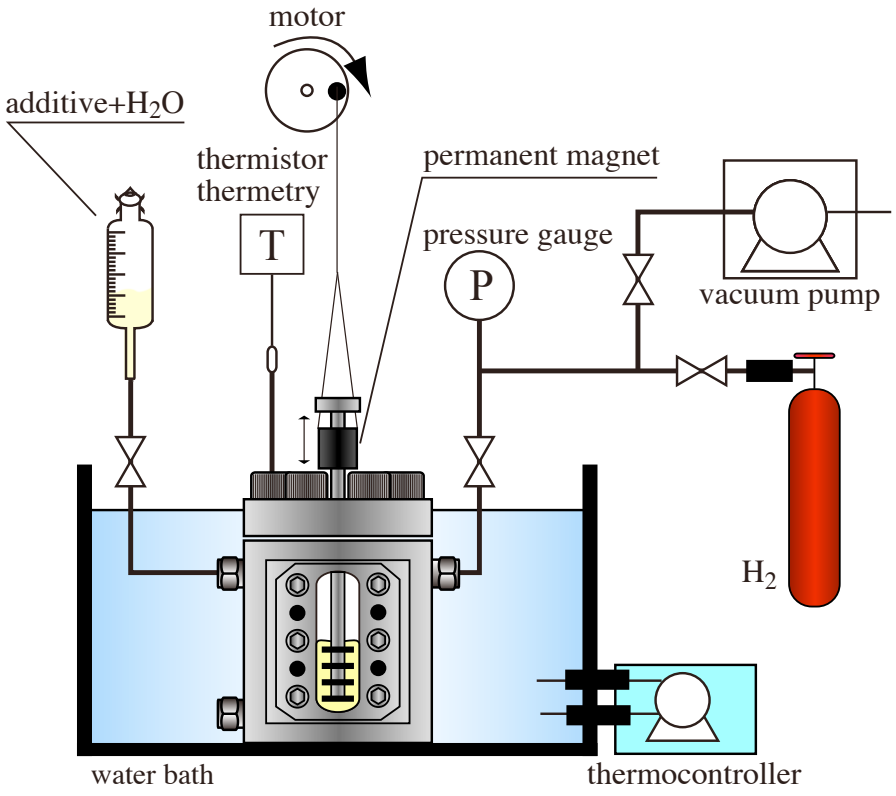

Fig. 2-1 Schematic illustration of experimental apparatus for phase equilibrium measurement (> 5 MPa).

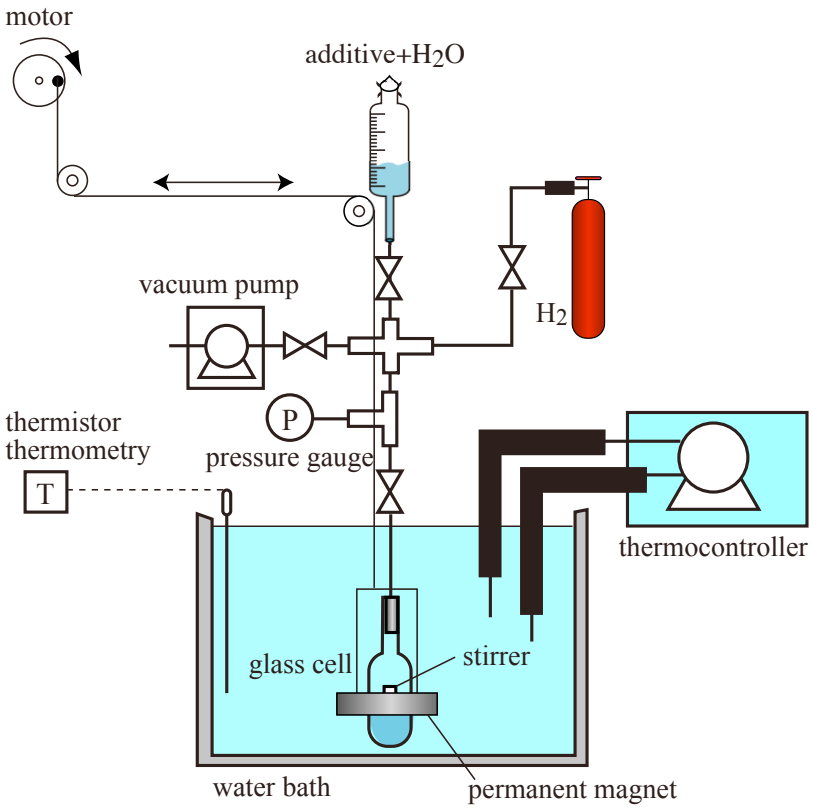

Fig. 2-2 Schematic illustration of experimental apparatus for phase equilibrium measurement (< 5 MPa).

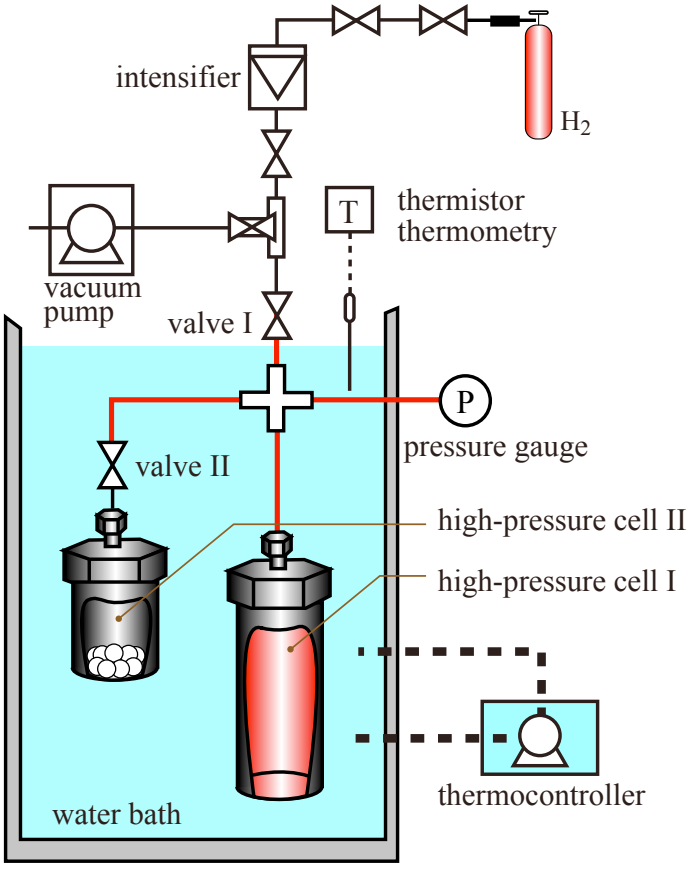

Fig. 2-3 Schematic illustration of experimental apparatus for *p*-*V*-*T* measurement.

2. 2. 2. Procedures

(a) Phase equilibrium measurement

The mixture of additive (THT, furan, or *c*-C_5H_{10} (non-hydrosoluble)) + water prepared at stoichiometric mole ratio for the s-II hydrate (feed mole ratio, additive : water = 1:17) was introduced into the high-pressure cell evacuated beforehand in several batches by use of the vacuum pump to remove dissolved air. The content was pressurized carefully up to a desired pressure by supplying H_2. In order to generate the mixed hydrate particle, the cell was cool down to 258 K and the contents were stirred continuously. The formation of gas hydrate can be confirmed through the window of the cell. After the first particle of H_2+additive mixed-gas hydrate was visually observed, the system temperature and agitation were kept constant during at least a day in order to establish the four-phase equilibrium state of gas, aqueous, liquid additive, and hydrate phases. After reaching the four-phase equilibrium state, the equilibrium temperature and pressure were measured. In order to eliminate a hysteresis effect, the same equilibrium measurements were repeated using the fresh mixture of additive+water at the same mole ratios.

(b) *p-V-T* measurement

Simple additive hydrates were generated by efficient agitation of the additive+water mixed liquid prepared at stoichiometric mole ratio, that were supercooled to ~270 K in a freezer. This temperature was same in the case of THF hydrate [6]. After complete formation of additive hydrate, it was annealed at the experimental temperature (~275.1 K (THT and furan hydrates) or ~277.1 K (*c*-C_5H_{10} hydrate)), which are little lower than the equilibrium temperature of each simple additive hydrates at atmospheric pressure for a day. Then, the hydrates were quenched and taken out from the cell at 263 K. These hydrates were crushed at 263 K with a mortar and pestle, and then sieved to the desired particle sizes of ~750 μm. Approximately 3 g of sieved additive hydrate was enclosed into the cell II that was cooled down in advance. The cell II was sealed and evacuated with being cooled in liquefied nitrogen. After that, the cell II was immersed in a temperature-controlled water bath at 275.1 K or 277.1 K. H_2 was introduced into the cell I up to a desired pressure and then the valve II was opened in order to pressurize the additive hydrates with H_2. The initial time was defined as the moment that valve II was opened and H_2 contacted with additive hydrate. The system pressure started dropping. After the system pressure reached at a constant value, the storage amount of H_2 was calculated from the amount of pressure change by use of equation of state. The volume ratio of both cells and virial coefficients were determined accurately by Burnett method [8]. In the present study, the mass% was defined as {H_2 / (H_2+ additive hydrates)}.

2. 2. 3. Materials

Research grade H_2 (mole fraction purity: 0.999999) was obtained from the Neriki Gas Co., Ltd. The maximum impurity was 0.2 ppm of nitrogen. Research grade THT (mole fraction purity: 0.99), furan (mole fraction purity: 0.99), and *c*-C_5H_{10} (mole fraction purity: 0.99) were obtained from Tokyo Chemical Industry, Co., Ltd. The distilled water was obtained from the Wako Pure Chemicals Industries, Ltd. All of them were used without further purifications.

2. 3. Results and Discussion

2. 3. 1. Thermodynamic Stability

Phase equilibrium relation for the H_2+THT, furan, or *c*-C_5H_{10} mixed hydrate systems are summarized in **Table 2-1** and shown in **Fig. 2-4**. Each mixed hydrate systems have four-phase equilibrium curves, and only H_2+THF mixed hydrate system has three-phase equilibrium curve. The phase behavior of each hydrate is similar to one another mixed hydrates, while the thermodynamic stability boundaries of H_2+THT, H_2+furan, H_2+THF, and H_2+*c*-C_5H_{10} hydrates are located in the order increasing the equilibrium temperature in **Fig. 2-4**.

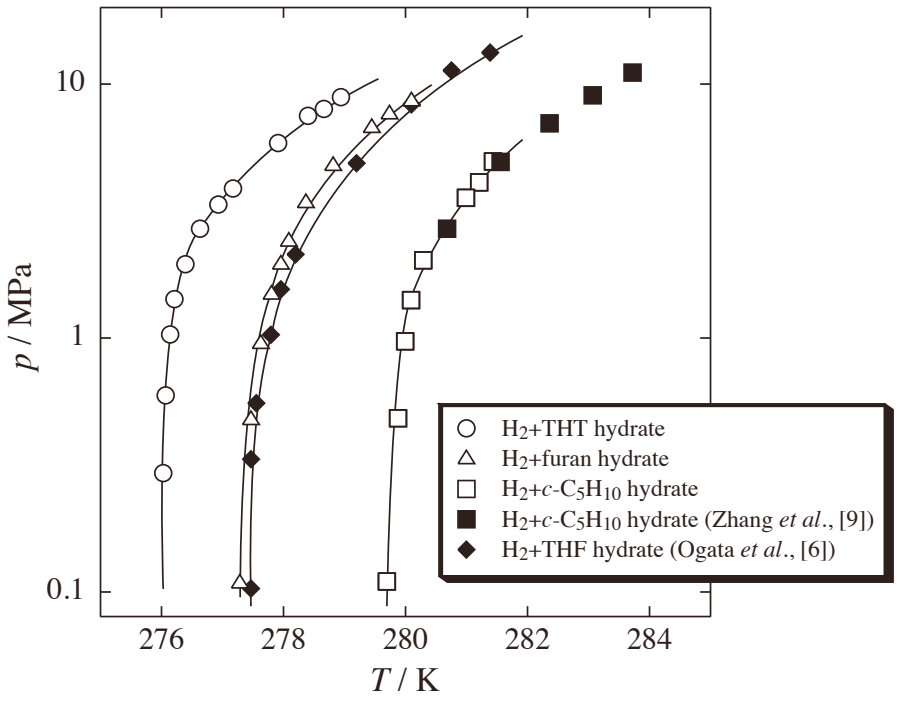

Fig. 2-4 Phase equilibrium (*p*-*T*) relations for the H_2+THT, furan, *c*-C_5H_{10}, and THF mixed hydrate systems. The solid lines are fitting lines for the experimental data.

Table 2-1 Four-phase equilibrium (*p*-*T*) data for the H_2+THT, furan, and *c*-C_5H_{10} mixed hydrate systems.

	***T* / K**	***p* / MPa**		***T* / K**	***p* / MPa**
H_2+THT	276.03	0.29	H_2+furan	277.96	1.98
	276.07	0.60		278.09	2.44
	276.14	1.03		278.37	3.47
	276.21	1.43		278.82	4.85
	276.39	1.96		279.45	6.85
	276.63	2.70		279.74	7.75
	276.93	3.35		280.10	8.71
	277.17	3.88			
	277.91	5.86	H_2+*c*-C_5H_{10}	279.69	0.11
	278.40	7.50		279.88	0.48
	278.66	7.99		279.99	0.97
	278.94	8.88		280.09	1.41
				280.29	2.02
H_2+furan	277.29	0.11		280.99	3.57
	277.47	0.48		281.21	4.11
	277.63	0.97		281.44	4.96
	277.81	1.51			

2. 3. 2. H_2 Storage Amount and Rate

The storage amounts of H_2 in THT, furan, and *c*-C_5H_{10} hydrates with various experimental pressures are shown in **Fig. 2-5** accompanied with the results of THF hydrate [6]. Hereafter, the storage amounts of H_2 in additive hydrate is represented as n_{H2} / $n_{add.}$, which is defined as (mole number of H_2 absorbed in additive hydrate) / (mole number of additive in hydrate). As shown in **Fig. 2-5**, the pressure dependence of n_{H2} / $n_{add.}$ exhibits the similar behavior to one another. Additionally, it would be inferred that n_{H2} / $n_{add.}$ reaches plateau at ~80 MPa and its value is 2.0, if the pressure dependence is the same as that of THF hydrate. This indicates that S-cage and L-cage are occupied by a single H_2 molecule and a single additive molecule, respectively.

Time variation of H_2 amount absorbed in the additive hydrates are shown in **Fig. 2-6**. Initial absorption rates of H_2 in additive hydrates become large with the increase of initial experimental pressure. That is, H_2 molecules begin to be absorbed in hydrate immediately after contact with the additive hydrate surface. This fact indicates that H_2 can diffuse almost freely through the hydrate cages [10, 11]. In the release process, the storage amount of H_2 is dropped to the equilibrium storage amount corresponding to the reduced pressures. Most importantly, H_2 can be absorbed and released reversibly by pressurizing or depressurizing without the destruction of hydrate cages in additive hydrate, based on the following: First, these hydrates are thermodynamically stable in the present experimental conditions. Second, H_2 molecule is captured in only S-cage while all L-cages are occupied by additive molecule. Third, 2nd storage with additive hydrates which released H_2 once exhibit similar behavior to the 1st storage with fresh one.

Figure 2-7 compares the time variation of n_{H2} / $n_{add.}$ under the similar pressure conditions. The initial experimental pressure was ~35 MPa. In the case of THT, furan, and *c*-C_5H_{10} hydrates, it takes approximately 3 hours for the H_2 absorption to reach to more than 90 % of the equilibrium storage amount of H_2. On the other hand, in the case of THF hydrate, H_2 absorption rate is smaller than that of the other hydrates despite almost the same temperature and pressure conditions. A longer period than 10 hours is required until *c*-C_5H_{10} hydrate absorbs H_2 up to the equilibrium storage amount as much as the THF hydrate, while it takes within 5 hours in the case of THT and furan hydrates.

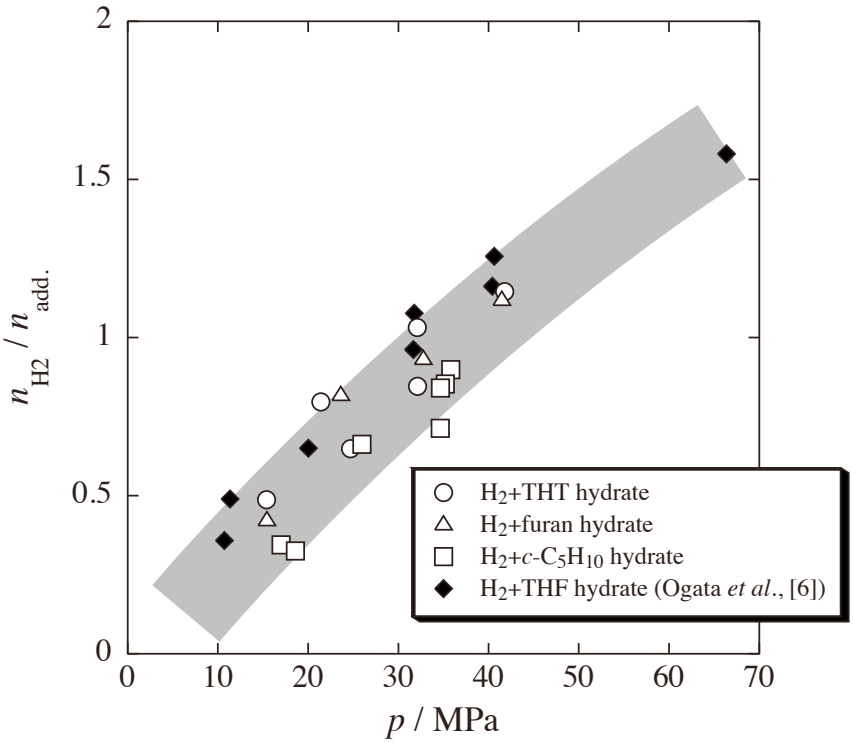

Fig. 2-5 The pressure dependence of H_2 storage amount in the THT hydrate at 275.1 K, furan hydrate at 275.1 K, *c*-C_5H_{10} hydrate at 277.1 K, and THF hydrate at 277.1 K. The shaded area represents the tendency of estimated n_{H2} / $n_{add.}$.

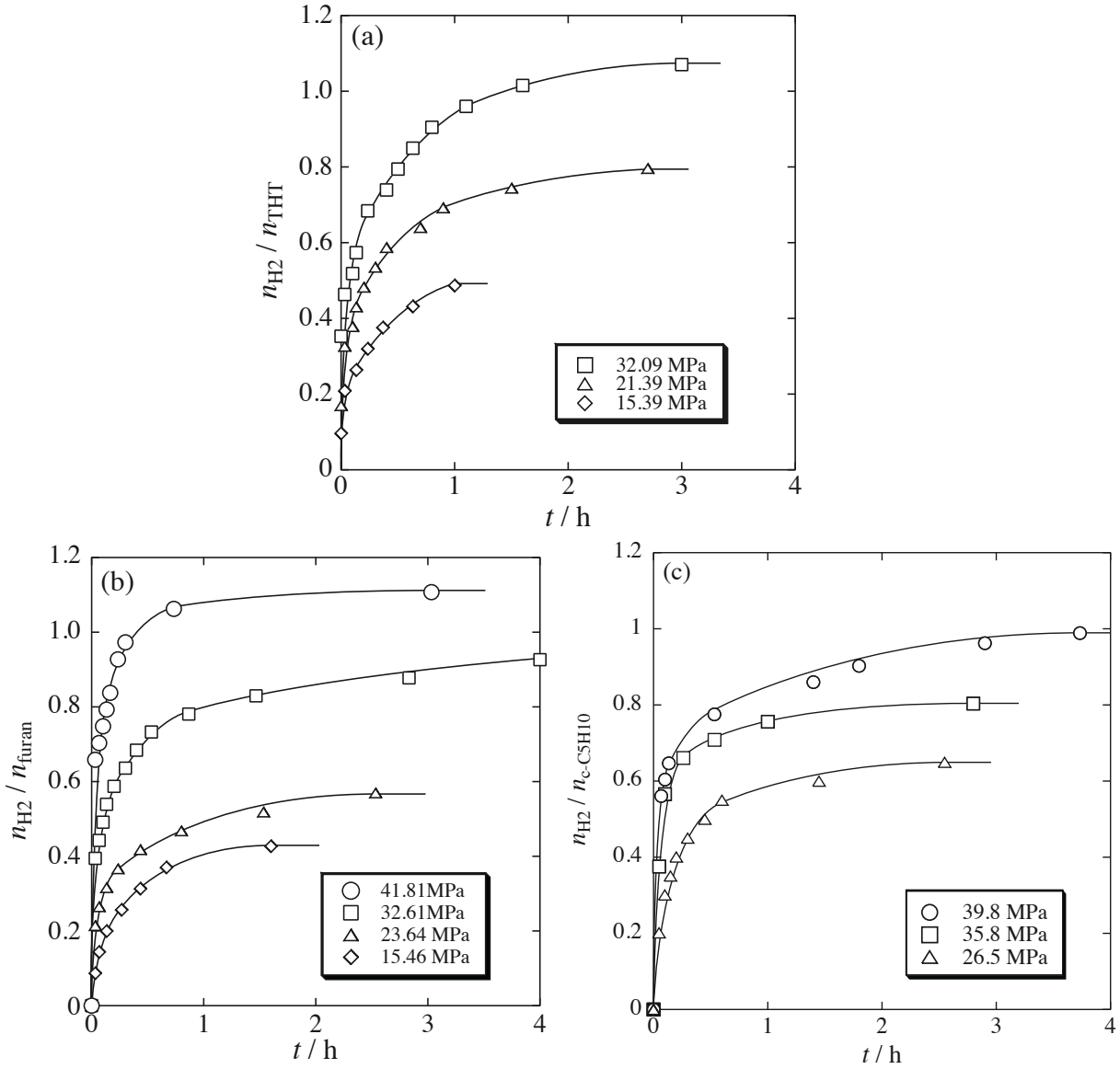

Fig. 2-6 Time variation of H_2 amount absorbed in THT hydrate (a) and furan hydrate (b) at 275.1 K, *c*-C_5H_{10} hydrate (c) at 277.1 K (the particle diameter of each hydrates is ~750 μm). The solid lines are fitting lines for experimental data.

As mentioned above, initial absorption rates of H_2 in THT, furan, and *c*-C_5H_{10} hydrate are larger than that of THF hydrate, while H_2 storage capacity is nearly equivalent to one another. This may be attributed to the expansion or distortion of hydrate cages, and physical and chemical properties of additives such as solubility. The detail, however, is still unclear.

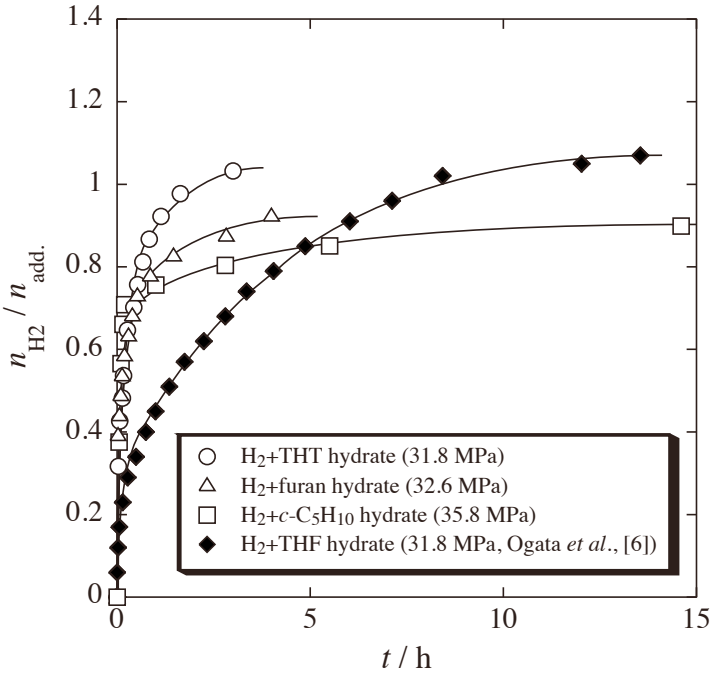

Fig. 2-7 Comparison of H_2 absorption rate among THT hydrate at 31.8 MPa, furan hydrate at 32.6 MPa, *c*-C_5H_{10} hydrate at 35.8 MPa, and THF hydrate at 31.8 MPa for same particle diameter of ~750 μm. The solid lines are fitting lines for experimental data.

2. 4. Conclusion

The storage capacities of H_2 in THT, furan, and *c*-C_5H_{10} hydrates have been investigated by means of *p-V-T* measurement. It is confirmed that the reversible storage and release processes of H_2 in THF, furan, and *c*-C_5H_{10} hydrates are feasible by pressurizing and depressurizing without the destruction of hydrate cages. The H_2 absorption rate of THT, furan, and *c*-C_5H_{10} hydrates is larger than that of THF hydrate while their storage amounts of H_2 are comparable.

Notation

n: mole number [mol]
p: pressure [Pa]
T: temperature [K]
t: time [h]

References

[1] Florusse, L. J.; Peters, C. J.; Schoonman, J.; Hester, K. C.; Koh, C. A.; Dec, S. F.; Marsh K. N.; Sloan, E. D. "Stable Low-Pressure Hydrogen Clusters Stored in a Binary Clathrate Hydrate.", *Science*, **306**, 469-471 (2004).

[2] Strobel, T. A.; Taylor, C. J.; Hester, K. C.; Dec, S. F.; Koh, C. A.; Miller, K. T.; Sloan, E. D., Jr. "Molecular Hydrogen Storage in Binary THF-H2 Clathrate Hydrates.", *Journal of Physical Chemistry B*, **110**, 17121-17125 (2006).

[3] Hashimoto, S.; Murayama, S.; Sugahara, T.; Sato, H.; Ohgaki, K. "Thermodynamic and Raman Spectroscopic Studies on H_2 + Tetrahydrofuran + Water and H_2 + Tetra-*n*-butyl Ammonium Bromide + Water Mixtures Containing Gas Hydrates.", *Chemical Engineering Science*, **61**, 7884-7888 (2006).

[4] Hashimoto, S.; Sugahara, T.; Sato, H.; Ohgaki, K. "Thermodynamic Stability of H_2 + Tetrahydrofuran Mixed Gas Hydrate in Nonstoichiometric Aqueous Solutions.", *Journal of Chemical & Engineering Data*, **52**, 517-520 (2007).

[5] Hashimoto, S.; Sugahara, T.; Moritoki, M.; Sato, H.; Ohgaki, K. "Thermodynamic Stability of Hydrogen + Tetra-*n*-Butyl Ammonium Bromide Mixed Gas Hydrate in Nonstoichiometric Aqueous Solutions.", *Chemical Engineering Sci*ence, **63(4)**, 1092-1097 (2008).

[6] Ogata, K.; Hashimoto, S.; Sugahara, T.; Moritoki, M.; Sato, H.; Ohgaki, K. "Storage Capacity of Hydrogen in Tetrahydrofuran Hydrate.", *Chemical Engineering Science*, **63(23)**, 5789-5794 (2008).

[7] Nagai, Y.; Yoshioka, H.; Ota, M.; Sato, Y.; Inomata, H.; Smith, R. L., Jr.; Peters, C. J. "Binary Hydrogen-Tetrahydrofuran Clathrate Hydrate Formation Kinetics and Models.", *AIChE Journal*, **54(11)**, 3007-3016 (2008).

[8] Katayama, T.; Ohgaki, K. "Measurement of Interaction Second Virial Coefficients with High Accuracy.", *Journal of Chemical Engineering of Japan*, **13**, 257-262 (1980).

[9] Zhang, J. S.; Lee, J. W. "Equilibrium of Hydrogen + Cyclopentane and Carbon Dioxide + Cyclopentane Binary Hydrates.", *Journal of Chemical & Engineering Data*, **54**, 659-661 (2009).

[10] Alavi, S.; Ripmeester, J. A.; "Hydrogen-Gas Migration through Clathrate Hydrate Cages.", *Angewandte Chemie, International Ed*ition, **46**, 6102-6105 (2007).

[11] Okuchi, T.; Moudrakovski, I. L.; Ripmeester, J. A. “Efficient Storage of Hydrogen Fuel into Leaky Cages of Clathrate Hydrate.”, *Applied Physics Letters*, **91**, 171903-1-3 (2007).

[12] Lee, H.; Lee, J. -W.; Kim, D. Y.; Park, J.; Seo, Y. -T.; Zeng, H.; Moudrakovski, I. L.; Ratcliffe, C. I.; Ripmeester, J. A. “Tuning Clathrate Hydrates for Hydrogen Storage.”, *Nature*, **434**, 743-746 (2005).

[13] Sugahara, T.; Haag, J. C.; Prasad, P. S. R.; Warntjes, A. A.; Sloan, E. D.; Sum, A. K.; Koh, C. A. “Increasing Hydrogen Storage Capacity Using Tetrahydrofuran.”, *Journal of the American Chemical Soc*iety, **131**, 14616-14617 (2009).

[14] Sugahara, T.; Haag, J. C.; Warntjes, A. A.; Prasad, P. S. R.; Sloan, E. D.; Koh, C. A.; Sum, A. K. “Large-Cage Occupancies of Hydrogen in Binary Clathrate Hydrates Dependent on Pressures and Guest Concentrations.”, *Journal of Physical Chemistry C*, **114**, 15218-15222 (2010).

Chapter 3

Thermodynamic Properties of Hydrogen + Tetra-*n*-Butyl Ammonium Bromide Semi-clathrate Hydrate

Abstract

Thermodynamic stability and hydrogen occupancy on the hydrogen + tetra-*n*-butyl ammonium bromide semi-clathrate hydrate were investigated by means of Raman spectroscopic and phase equilibrium measurements under the three-phase equilibrium condition. The structure of mixed hydrates changes from tetragonal to another structure around 95 MPa and 292 K depending on surrounding hydrogen fugacity. The occupied amount of hydrogen in the semi-clathrate hydrate increases significantly associated with the structural transition. Tetra-*n*-butyl ammonium bromide semi-clathrate hydrates can absorb hydrogen molecules by a pressure-swing without destroying the hydrogen bonds of hydrate cages at 15 MPa or over.

Keywords: Gas hydrate, Phase equilibria, Stability, Cage occupancy, High pressure, Absorption

3. 1. Introduction

The hydrate formed from tetra-*n*-butyl ammonium salt solution has been known as a semi-clathrate hydrate where the quaternary ammonium cation and anion are incorporated with the water molecules to construct the hydrate cage [1]. It is reported that tetra-*n*-butyl ammonium salts can form various unit-cell structures. For example, tetra-*n*-butyl ammonium bromide (hereafter, TBAB) forms two unit-cell structures (tetragonal and orthorhombic) depending on the concentration of aqueous solution [2, 3]. In our previous study, the cage occupancy of H_2 has been investigated by use of phase equilibrium measurements and Raman spectroscopic analyses for two structures of H_2+TBAB semi-clathrate hydrates up to 15 MPa [4].

In Chapter 3, there are two research objectives: (1) thermodynamic property including hydrate structures and H_2 occupancy and (2) capability of reversible storage and release and storage capacity of H_2. Firstly, the cage occupancy of H_2 and structural transition for the H_2+TBAB semi-clathrate hydrate under the three-phase equilibrium conditions were investigated by means of *in situ* Raman spectroscopy. Secondly, phase equilibrium (pressure-temperature) relations for the ternary mixtures of H_2+TBAB+water at two TBAB concentrations were measured in the pressure region of 15-190 MPa. Finally, the capability of reversible storage and release of H_2 was evaluated by *in situ* Raman spectroscopic analysis using isothermal pressure-swing.

3. 2. Experimental

3. 2. 1. Apparatus

All apparatus are the same ones and details are shown in Chapters 1 and 2.

3. 2. 2. Procedures

(a) Phase equilibrium measurement

The aqueous TBAB solution prepared at a desired concentration (x = 0.037 which is the stoichiometric concentration of tetragonal TBAB hydrate, or 0.020 which is lower than the stoichiometric concentration of orthorhombic TBAB hydrate [2]) was introduced into the evacuated high-pressure optical cell. The contents were pressurized up to a desired pressure by supplying H_2 and then cooled and agitated with an enclosed ruby ball to prepare the gas hydrate. After the formation of

gas hydrates, the system temperature was risen gradually (about 0.1 K/hour) to leave a few seed crystals. In this state, the system temperature was kept constant for more than one day, and the three-phase equilibrium condition was determined. Preparing single crystal of gas hydrate and analyzing by means of Raman spectroscopy are same as shown in Chapter 1.

(b) Storage capacity of H_2

In the isothermal Raman spectroscopic measurement, an aqueous TBAB solution prepared with $x = 0.037$ was introduced into the evacuated high-pressure optical cell. To prepare the TBAB hydrate, the contents were supercooled and agitated with an enclosed ruby ball. After the formation of gas hydrates, the system temperature was kept constant, and the contents were annealed for more than one day at 283.15 K to complete the hydrate crystallization, which was slightly lower than the equilibrium temperature of TBAB hydrate at atmospheric pressure. Then, the contents were pressurized up to a desired pressure by supplying H_2, and the cell was kept static to establish the two-phase (H_2 gas and hydrate phases) equilibrium state. After one day, the hydrate phase was analyzed under the isothermal condition (283.15 K) through a sapphire window by *in situ* Raman spectroscopy.

In addition, the H_2+TBAB hydrate was prepared from compressed H_2 and aqueous solution in advance, and H_2 was once released from the H_2+TBAB hydrate at 283.15 K by depressurization. Then, the TBAB hydrate was pressurized again up to a desired pressure with H_2, and after one day or more, the hydrate was analyzed under isothermal two-phase equilibrium condition by *in situ* Raman spectroscopy. For convenience, the description of “repressurizing method” is adopted hereafter in this thesis.

3. 2. 3. Materials

Research grade H_2 (mole fraction purity: 0.999999) was obtained from the Neriki Gas Co., Ltd. The maximum impurity was 0.2 ppm of nitrogen. Research grade TBAB (mole fraction purity: 0.98) and the distilled water was obtained from the Wako Pure Chemicals Industries, Ltd. All of them were used without further purifications.

3. 3. Results and Discussion

3. 3. 1. Thermodynamic Property

The Raman spectra for the H_2+TBAB semi-clathrate hydrate system under the three-phase equilibrium condition are shown in **Figs. 3-1** (x = 0.037) and **3-2** (x = 0.020). The characteristic Raman peaks derived from TBAB molecule are detected around 700-1500 cm^{-1} and 2800-3000 cm^{-1} in the hydrate phase. The figures also include the single peak (4132 cm^{-1}) of H_2 stretching vibration and the broad peak (around 3100 cm^{-1}) corresponding to the O–H vibration of host water lattice for the H_2+TBAB semi-clathrate hydrate. The H_2 vibration peak is normalized by use of one of TBAB peaks. The position and shape of the peak derived from H_2 obtained in the present study agree well with those of previous reports [4, 5]. The Raman spectra reveal that the H_2 selectively occupies the empty S-cages of semi-clathrate hydrate, while the butyl-group of TBAB molecule occupies the other cages completely under the present experimental conditions.

Normalized peak of H_2 vibration becomes larger and larger with the pressure increasing, which means the increase of entrapped H_2 molecules. As shown in **Fig. 3-1**, in the case of x = 0.037, Raman peak ratio of H_2 to TBAB increases gradually as pressure increasing until *ca*. 100 MPa, while the increment of H_2 peak with pressure increasing seems to become small in the higher-pressure region.

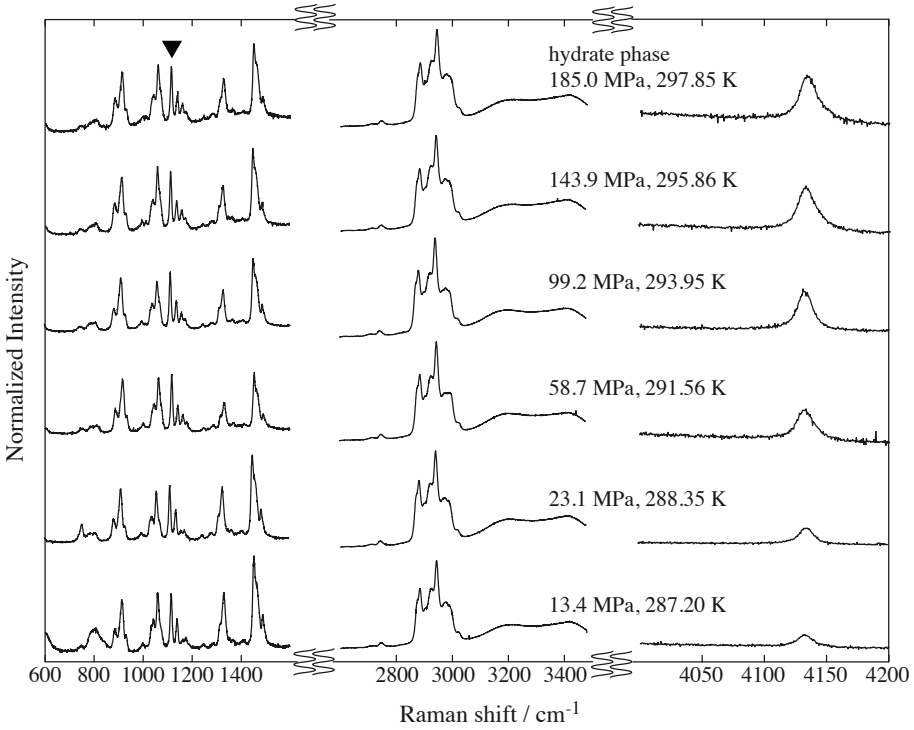

Fig. 3-1 Raman spectra originated from TBAB, H_2, and host lattice of water in the H_2+TBAB semi-clathrate hydrate with x = 0.037. Closed inverted-triangle represents the peak used for the normalization of H_2 vibration peak.

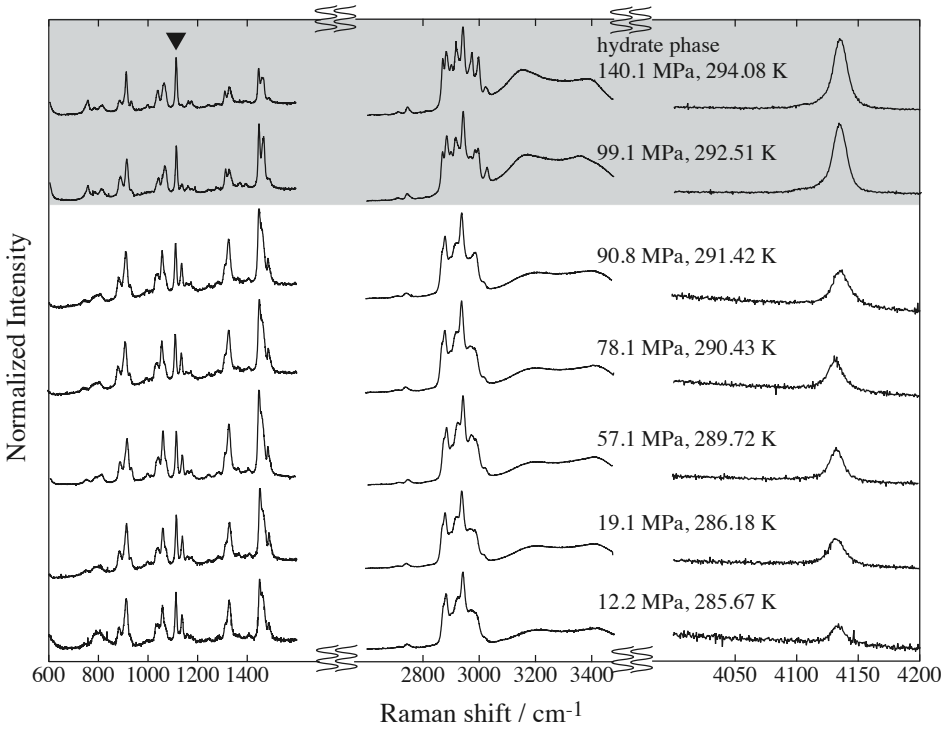

Fig. 3-2 Raman spectra originated from TBAB, H_2, and host lattice of water in the H_2+TBAB semi-clathrate hydrate with $x = 0.020$. Closed inverted-triangle represents the peak used for the normalization of H_2 vibration peak.

Table 3-1 Three-phase equilibrium conditions of H_2+TBAB semi-clathrate hydrate at the TBAB mole fraction of 0.020 and 0.037 in high-pressure region. The conditions in low-pressure are shown in the previous papers [4, 5]. x represents the mole fraction of TBAB aqueous solution.

	***T* / K**	***p* / MPa**		***T* / K**	***p* / MPa**
$x = 0.020$	286.45	19.5	$x = 0.037$	288.35	23.1
	288.23	35.6	tetragonal	291.56	58.7
	290.07	58.0		293.95	99.2
↑	290.97	78.8		295.86	143.9
tetragonal	291.53	91.6		297.85	185.0
new structure	292.87	101.3			
↓	294.75	140.6			

On the other hand, in the case of $x = 0.020$, Raman peak ratio of H_2 changes discontinuously around 100 MPa as shown in **Fig. 3-2** (shaded region). The normalized peak area of H_2 in the case of $x = 0.020$ increases dramatically compared with that of $x = 0.037$ at similar pressure more than 99 MPa. In

addition, the Raman peaks of TBAB and water change significantly on reaching *ca*. 100 MPa in x = 0.020, which differs in results from the case of x = 0.037. The peaks of TBAB at high pressures in x = 0.020 are closely similar to those of the other structure (probably orthorhombic) obtained in our previous study [4]. The orthorhombic structure (TBAB·38H_2O) [3] has more empty S-cages and can entrap much more H_2 than the tetragonal one (TBAB·26H_2O).

The phase equilibrium (pressure-temperature) relations for the H_2+TBAB semi-clathrate hydrate systems are summarized in **Table 3-1** and shown in **Fig. 3-3**. The three-phase equilibrium curves obtained in the present study join smoothly with those of our previous data [4, 5]. The characteristic slope change (dp/dT) derived from the structural transition on the three-phase equilibrium curve exists at ~95 MPa and 292 K only in the case of x = 0.020.

3. 3. 2. Storage Capacity of H_2

Raman spectroscopy exhibits that H_2 can be absorbed in TBAB hydrates without destroying the hydrogen bonds of hydrate cages at 15 MPa or over by use of isothermal pressure-swing. The results from "repressurizing method" (please refer to the experimental section for details) are shown in **Fig. 3-4** accompanied with those of Raman spectroscopic measurement under the stability boundary

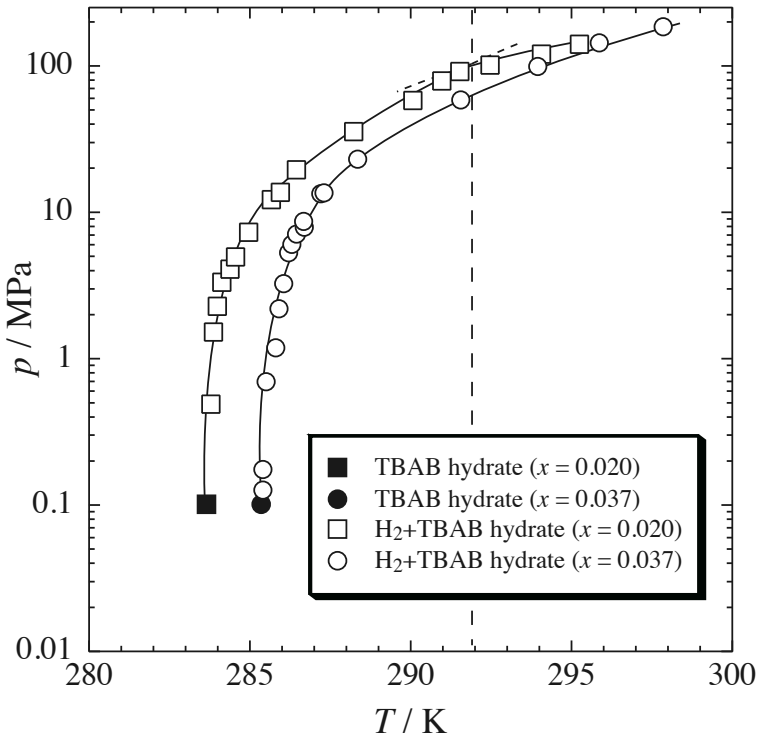

Fig. 3-3 Three-phase equilibrium curves of the H_2+TBAB semi-clathrate hydrates; closed keys represent the three-phase equilibrium points of simple TBAB semi-clathrate hydrates under the atmospheric conditions. The solid lines are fitting lines for experimental data.

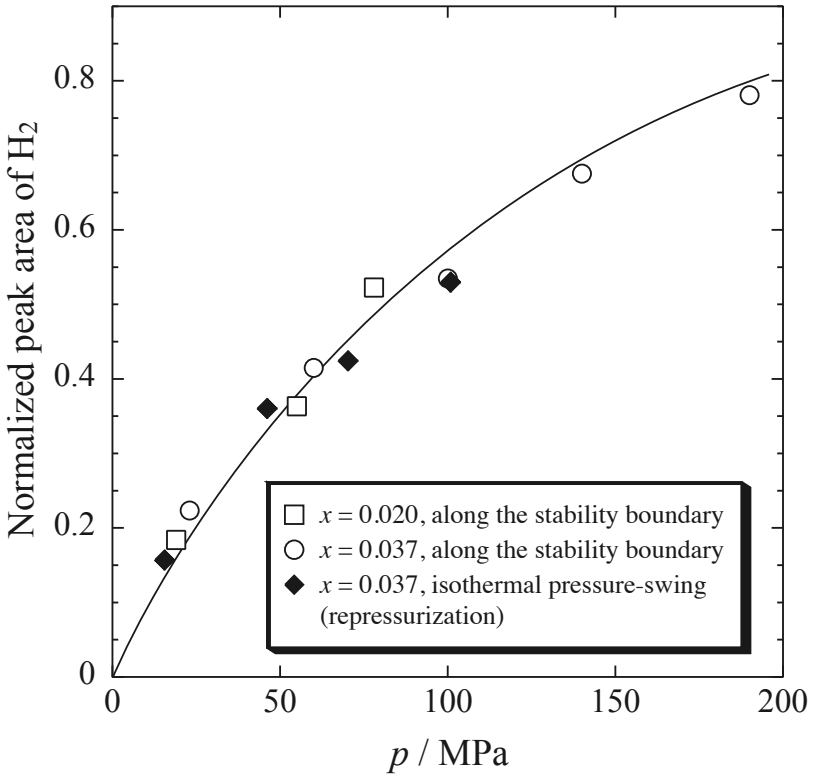

Fig. 3-4 Pressure dependence of normalized Raman peak area of H_2 in the H_2+TBAB semi-clathrate hydrate system.

conditions. The *y*-axis represents the peak area of H_2 normalized by one of peaks corresponding to TBAB molecule. As shown in **Fig. 3-4**, normalized Raman peak area of H_2 resulted from isothermal pressure-swing increases gradually as pressure rises and is coincident with the H_2 peak area measured under the stability boundary conditions. In the case of H_2 absorption to fresh TBAB hydrate, Raman peak area of H_2 reaches only about 70 % of the value obtained from "repressurizing method" at the same pressure. These results disagree with those of s-II THF hydrate system [6]. The discrepancy in hydrate structures results in that H_2 cannot diffuse freely in fresh TBAB hydrate because the empty S-cages do not connect successively. In the case of "repressurizing method," the release of H_2 from H_2+TBAB hydrate induces the secondary structural change of TBAB hydrate; for example, the position of nitrogen or bromine atom connected with host water may be changed. In fact, the crystal appearance of TBAB hydrate changes from clear to cloudy at the moment H_2 released from H_2+TBAB hydrate. The secondary TBAB hydrate prepared by H_2 release from H_2+TBAB hydrate may enable us to perform the reversible H_2 storage and release. **Figure 3-4** also shows that the normalized peak area of H_2 is not saturated even if the pressure reaches about 200 MPa; that is, the empty S-cages cannot be occupied completely by H_2 at least 200 MPa.

3. 4. Conclusion

The thermodynamic stability and H_2 occupancy for the H_2+TBAB semi-clathrate hydrate system were investigated by phase equilibrium (pressure-temperature) relation and Raman spectra measured at two mole fractions (x = 0.020 or 0.037) of TBAB aqueous solution. In the case of x = 0.020, the structural transition from tetragonal to another structure occurs around 95 MPa and 292 K. The structure can store much more H_2 molecules than the tetragonal one. Raman spectroscopic analysis with isothermal pressure-swing absorption reveals that H_2 can be absorbed in the TBAB hydrates without destroying the hydrogen bonds of hydrate cages. The storage amount of H_2 for the repressurization to the used TBAB hydrate after H_2 release increases compared with that of fresh TBAB hydrate. It remains possible to perform the reversible storage and release of H_2 in TBAB hydrate without destroying hydrate cages.

Notation

p: pressure [Pa]
T: temperature [K]
x: mole fraction of TBAB in the aqueous solution [-]

References

[1] Aladko, L. S.; Dyadin, Y. A.; Rodionova, T. V.; Terekhova, I. S. "Clathrate Hydrates of Tetrabutylammonium and Tetraisoamylammonium Halides.", *Journal of Structural Chemistry*, **43(6)**, 990-994 (2002).

[2] Shimada, W.; Ebinuma, T.; Oyama, H. "Separation of Gas Molecule Using Tetra-*n*-butyl Ammonium Bromide Semi-clathrate Hydrate Crystals.", *Japanese Journal of Applied Physics*, **42**, L129-L131 (2003).

[3] Shimada, W.; Shiro, M.; Kondo, H.; Takeya, S.; Oyama, H.; Ebinuma, T.; Narita, H. "Tetra-*n*-butylammonium Bromide-Water (1/38).", *Acta Crystallographica Section C*, **C61**, o65-o66 (2005).

[4] Hashimoto, S.; Sugahara, T.; Moritoki, M.; Sato, H.; Ohgaki, K. "Thermodynamic Stability of Hydrogen + Tetra-*n*-Butyl Ammonium Bromide Mixed Gas Hydrate in Nonstoichiometric Aqueous Solutions.", *Chemical Engineering Sci*ence, **63(4)**, 1092-1097 (2008).

[5] Hashimoto, S.; Murayama, S.; Sugahara, T.; Sato, H.; Ohgaki, K. "Thermodynamic and Raman Spectroscopic Studies on H_2 + Tetrahydrofuran + Water and H_2 + Tetra-*n*-butyl Ammonium Bromide + Water Mixtures Containing Gas Hydrates.", *Chemical Engineering Science*, **61**, 7884-7888 (2006).

[6] Ogata, K.; Hashimoto, S.; Sugahara, T.; Moritoki, M.; Sato, H.; Ohgaki, K. "Storage Capacity of Hydrogen in Tetrahydrofuran Hydrate.", *Chemical Engineering Science*, **63(23)**, 5789-5794 (2008).

Chapter 4

Thermodynamic Properties of Hydrogen + Tetra-*n*-Butyl Ammonium Fluoride Semi-clathrate Hydrate

Abstract

Thermodynamic stability and hydrogen occupancy on the hydrogen + tetra-*n*-butyl ammonium fluoride semi-clathrate hydrate have been investigated by means of phase equilibrium (pressure-temperature) measurements and Raman spectroscopic analyses for two mole fractions,0.018 and 0.034 (stoichiometric for the cubic structure) of tetra-*n*-butyl ammonium fluoride aqueous solutions. In the case of $x = 0.034$, the stability boundary curve of hydrogen + tetra-*n*-butyl ammonium fluoride semi-clathrate hydrate locates at about 23 K higher temperature than that of hydrogen + tetrahydrofuran mixed hydrate, while the storage capacity of hydrogen is smaller. In the case of hydrate prepared from the $x = 0.018$ of aqueous solution, the Raman spectra and phase behavior reveal that the cubic structure of semi-clathrate hydrate is changed to a different one at about 9 MPa and 299.2 K. The new structure can entrap larger amount of hydrogen than the cubic one. The stability boundary curve of hydrogen + tetra-*n*-butyl ammonium fluoride semi-clathrate hydrate obtained in the aqueous solution of $x = 0.018$ is shifted to slightly low-temperature or high-pressure side from that of $x = 0.034$.

Keywords: Gas hydrate, Phase equilibria, Stability, Gas storage, Solutions, Gases

4. 1. Introduction

Most recently, tetra-*n*-butyl ammonium salts have become the object of much attention as an attractive additive [1, 2], for example, tetra-*n*-butyl ammonium bromide (hereafter, TBAB) and fluoride (hereafter, TBAF). Simple TBAB or TBAF hydrate has been known as a semi-clathrate hydrate where the quaternary ammonium cation and halogen anion of these salts are incorporated with the water molecules to construct the hydrate cage. There are various reports about the crystal structure and the role of halogen anion in these semi-clathrate hydrates [3-6]. In our previous study, the cage occupancy of H_2 has been revealed by use of phase equilibrium measurements and Raman spectroscopic analyses for two structures of H_2+TBAB mixed hydrates [7]. TBAF hydrate can exist at room temperature [3, 8], which is far higher than the equilibrium temperature of TBAB hydrate. Hence, TBAF hydrate is favorable as a storehouse of H_2 [2]. It is necessary to investigate both the phase behavior and H_2 occupancy in the H_2+TBAF semi-clathrate hydrate system.

In Chapter 4, phase equilibrium (pressure-temperature) relations for the H_2+TBAF+water ternary mixtures at two TBAF concentrations were measured. In addition, the cage occupancy of H_2 in the H_2+TBAF semi-clathrate hydrate under the three-phase equilibrium states were investigated by means of *in situ* Raman spectroscopy.

4. 2. Experimental

4. 2. 1. Apparatus

All apparatus are the same ones and details are shown in Chapters 1 and 2.

4. 2. 2. Procedures

(a) Phase equilibrium measurement

Experimental procedures of phase equilibrium measurements are same shown in Chapter 3, except for the mole fraction of TBAF aqueous solution, which is 0.018 or 0.034. The latter one is the stoichiometric concentration of TBAF semi-clathrate hydrate.

(b) Raman spectroscopic analyses

Experimental procedures of Raman spectroscopic analyses are same shown in Chapter 3, except for the mole fraction of TBAF aqueous solution. In the present study, the isothermal experiment has been not conducted.

4. 2. 3. Materials

Research grade H_2 (mole fraction purity: 0.999999) was obtained from the Neriki Gas Co., Ltd. The maximum impurity was 0.2 ppm of nitrogen. Research grade TBAF hydrate (mole fraction purity: 0.980), which was not semi-clathrate hydrate, was obtained from the Wako Pure Chemicals Industries, Ltd. The weight water content of general TBAF hydrate was ~17 mass%, which was analyzed by means of Karl Fisher's method. In the following section, the original water content of reagent is taken into consideration for the data analyses. The distilled water was obtained from the Wako Pure Chemicals Industries, Ltd. All of them were used without further purifications.

4. 3. Results and Discussion

4. 3. 1. Thermodynamic Property

In the present study, the phase equilibrium (temperature-composition) relation for the simple TBAF hydrate systems was also measured under the atmospheric conditions. The equilibrium data are shown in **Fig. 4-1** and summarized in **Table 4-1**. There are various reports about the structure of simple TBAF hydrate [3, 8, 9]. There are two structures of simple TBAF hydrate [3, 8]. The one is cubic structure ($TBAF{\cdot}28.6H_2O$), and the other is tetragonal structure ($TBAF{\cdot}32.3H_2O$), which seems to be a metastable structure. As shown in **Fig. 4-1**, TBAF hydrate is the most stable when the mole fraction of aqueous solution is $x = 0.034$ ($TBAF{\cdot}28.6 \pm 0.3H_2O$), where the equilibrium temperature is 300.75 K. The maximum equilibrium temperature and mole ratio of TBAF to H_2O for TBAF hydrate agree well with the result of Dyadin *et al*. [8] or Aladko *et al*. [3]. There is no stepwise variation of equilibrium curve that indicates the possibility of structural transition under the present experimental conditions.

Phase equilibrium (pressure-temperature) relations for the H_2+TBAF semi-clathrate hydrate systems at two TBAF concentrations ($x = 0.034$ or 0.018) are summarized in **Table 4-2** and shown in **Fig. 4-2**. The former concentration is the stoichiometric one for the cubic TBAF hydrate, and the latter is a smaller one than that of tetragonal TBAF hydrate ($x = 0.030$). The three-phase equilibrium curves

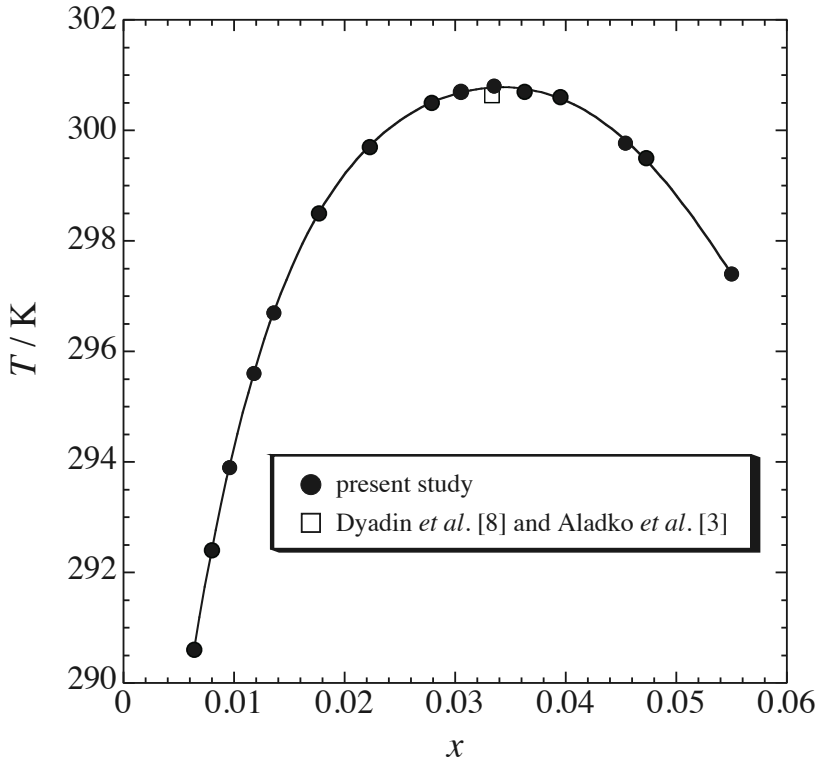

Fig. 4-1 Phase equilibrium (*T*-*x*) relation for the simple TBAF system under atmospheric conditions.

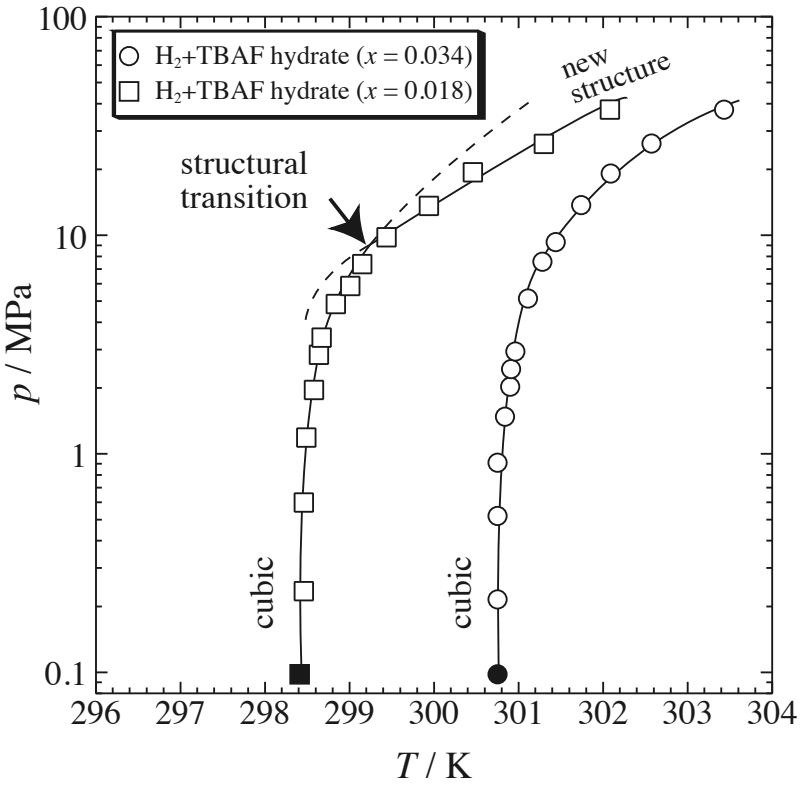

Fig. 4-2 Three-phase equilibrium curves of the H_2+TBAF semi-clathrate hydrate; closed keys represent the three-phase equilibrium point under the atmospheric conditions (corresponding to **Fig. 4-1**). The solid lines are fitting lines for experimental data.

Table 4-1 Phase equilibrium data for TBAF+water mixed system in the presence of hydrate phase at atmospheric pressure.

x	T / K	x	T / K
0.006	290.55	0.031	300.65
0.008	292.35	0.034	300.75
0.010	293.86	0.036	300.66
0.012	295.58	0.040	300.55
0.014	296.72	0.045	299.77
0.018	298.46	0.047	299.46
0.022	299.72	0.055	297.35
0.028	300.48	0.034 [3, 8]	300.55 [3, 8]

Table 4-2 Experimental dissociation conditions of H_2+TBAF semi-clathrate hydrate at the TBAF mole fraction of 0.018 and 0.034.

	T / K	p / MPa		T / K	p / MPa
x = 0.018	298.46	0.24	x = 0.034	300.75	0.22
	298.46	0.60	cubic	300.75	0.52
	298.49	1.19		300.75	0.91
	298.58	1.96		300.84	1.48
	298.64	2.83		300.90	2.03
	298.67	3.39		300.91	2.44
	298.84	4.84		300.96	2.94
↑	299.01	5.86		301.11	5.14
cubic	299.15	7.38		301.28	7.57
new structure	299.44	9.79		301.44	9.30
↓	299.94	13.6		301.74	13.8
	300.46	19.4		302.09	19.2
	301.30	26.2		302.57	26.3
	302.10	37.6		303.43	37.6

of H_2+TBAF semi-clathrate hydrate converge at the vicinity of each atmospheric equilibrium temperature (298.46 K and 300.75 K) of simple TBAF hydrate prepared from the same mole fraction solution, respectively. Each equilibrium curve vertically rises up in the pressure up to about 2 MPa, which may be attributed to the hydrogen content in the hydrate. Each three-phase equilibrium pressure increases continuously with the temperature increasing. The phase behavior obtained in the present study is similar to that of the data measured by Chapoy *et al*. [2]. The three-phase equilibrium curve obtained at the $x = 0.018$ is shifted to lower-temperature side than that of $x = 0.034$. Interestingly, there seems to be the characteristic slope change (dp/dT) of three-phase equilibrium curve at about 9 MPa only in the case of $x = 0.018$. These results imply the structural transition induced by the H_2 occupancy.

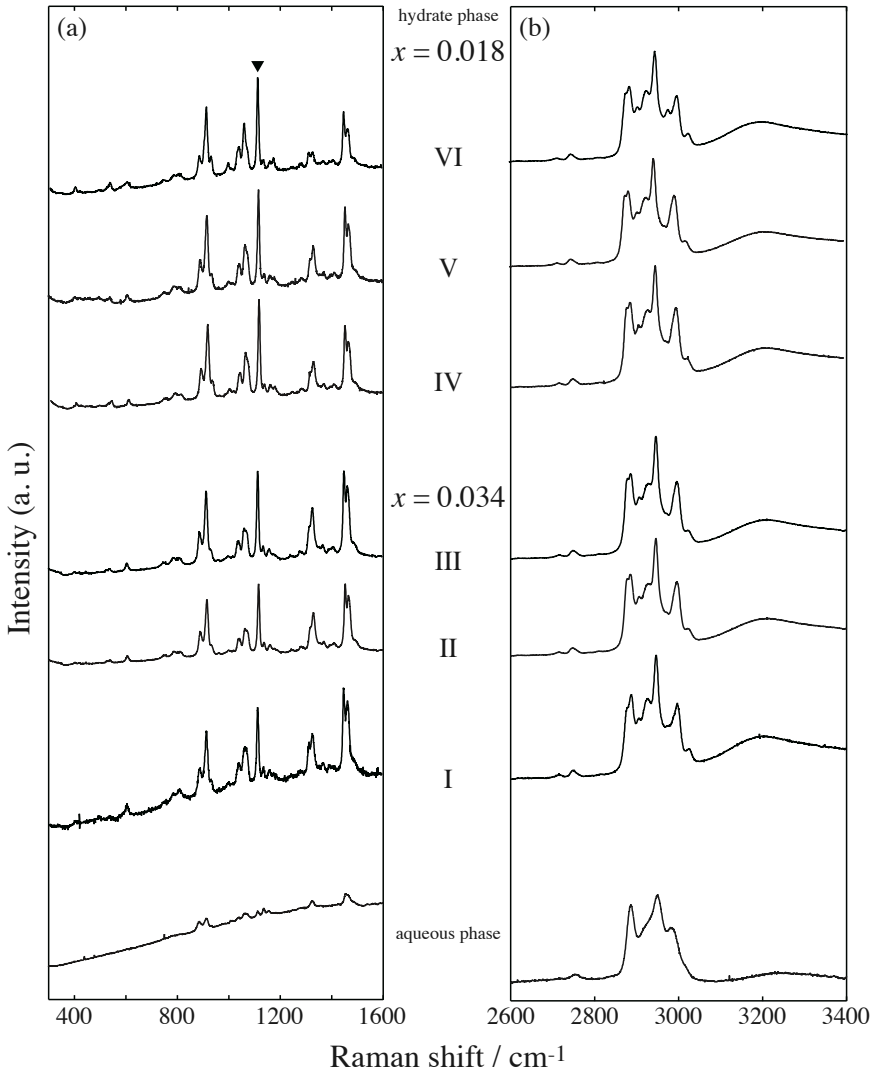

Fig. 4-3 Typical Raman spectra originated in TBAF in the aqueous and hydrate phases for the H_2+TBAF semi-clathrate hydrate system in the low (a) and high (b) wavenumber ranges. In the hydrate phase; ($x = 0.034$) I: 301.28 K, 7.57 MPa; II: 301.69 K, 11.3 MPa; III: 303.49 K, 38.1 MPa; ($x = 0.018$) IV: 299.15 K, 7.38 MPa; V: 299.94 K, 13.6 MPa; VI: 301.72 K, 34.7 MPa. Closed inverted-triangle represents the peak used for the normalization of H_2 vibration peak.

4. 3. 2. Raman Spectroscopic Analysis

The Raman spectra for the H_2+TBAF semi-clathrate hydrate system under the three-phase equilibrium state are shown in **Figs. 4-3** and **4-4**. The characteristic Raman peaks derived from TBAF molecule are detected around 700-1500 cm^{-1} and 2800-3000 cm^{-1} in the aqueous and hydrate phases. **Fig. 4-3** shows the typical Raman spectra of TBAF molecule for the H_2+TBAF semi-clathrate hydrate system. **Figure 4-3(b)** includes the broad peak corresponding to the O–H vibration of host water lattice. The spectra obtained in hydrate phase are distinct from those of aqueous solution phase. On the other hand, there is no remarkable change of Raman spectra depending on the variation of TBAF concentration or system pressure for the H_2+TBAF semi-clathrate hydrate.

The spectra of H_2 vibration for the H_2+TBAF semi-clathrate hydrate are shown in **Fig. 4-4**. These peaks are normalized with one of peaks derived from TBAF molecule. A broad single peak is detected at 4132 cm^{-1} in the hydrate phase. The position and shape of the peak derived from H_2 obtained in the present study agree well with those of H_2+TBAB semi-clathrate hydrate [1, 7]. The Raman spectra reveal that the cage selectivity of H_2 for the H_2+TBAF semi-clathrate hydrate is independent of both the TBAF concentrations in the aqueous solutions and the system pressures under the present experimental conditions. The H_2 selectively occupies the empty small cages of semi-clathrate hydrate, while the butyl-group of TBAF molecule occupies the other cages completely. In addition, normalized peak of H_2 vibration becomes larger with the pressure increasing, which means the increase of entrapped H_2 molecules. In the case of x = 0.034, Raman peak ratio of H_2 to TBAF increases gradually with the increase of system pressure. On the other hand, in the case of x = 0.018, Raman peak ratio of H_2 to TBAF changes dramatically at 13.6 MPa compared with those of 7.38 MPa. The normalized peak area of H_2 in the case of x = 0.018 increases dramatically compared with that of x = 0.034 at similar pressure.

Figure 4-5 shows the photographs of H_2+TBAF semi-clathrate hydrate crystals. The crystal appearances of x = 0.034 would be testudinal and do not change with the increase of system pressure. On the other hand, in the case of x = 0.018, the appearance of crystal changes from testudinal (7.38 MPa) to columnar (34.7 MPa). This indicates the crystallographic difference between two crystals prepared from different pressures. The appearance of simple TBAF hydrate for the aqueous solution of x = 0.034 resembles that of H_2+TBAF semi-clathrate hydrate crystal under the low-pressure regions. From the preliminary single-crystal X-ray scattering measurement at atmospheric pressure, it has been directly confirmed that the unit-cell structure of simple TBAF hydrate prepared from the aqueous solution of x = 0.034 is cubic (a = 2.44 nm, space group is Im3m), which agrees well with the previous data [3]. The cubic structure is known as an eight fold unit-cell of general structure-I, that is, it consists of 16 S-cages and 48 M-cages. Most recently, a new cubic structure (a = 2.4375 nm, space group is $I43d$, TBAF·29.7H_2O) has been reported [9]. The reason why there is the discrepancy between these two reports is unclear. However, it is reasonable to speculate the unit-cell structure of H_2+TBAF semi-clathrate hydrate prepared from the aqueous solution (x = 0.034) is also cubic.

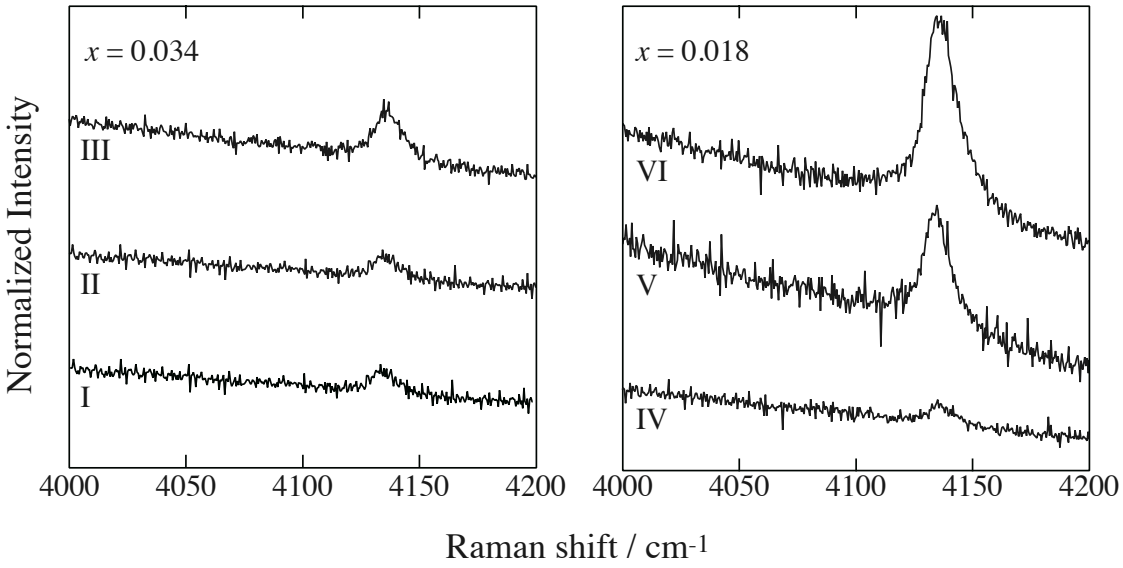

Fig. 4-4 Raman spectra corresponding to the intramolecular vibration of H_2 in the hydrate phase at two TBAF mole fractions. Each label corresponds to that of **Fig. 4-3**.

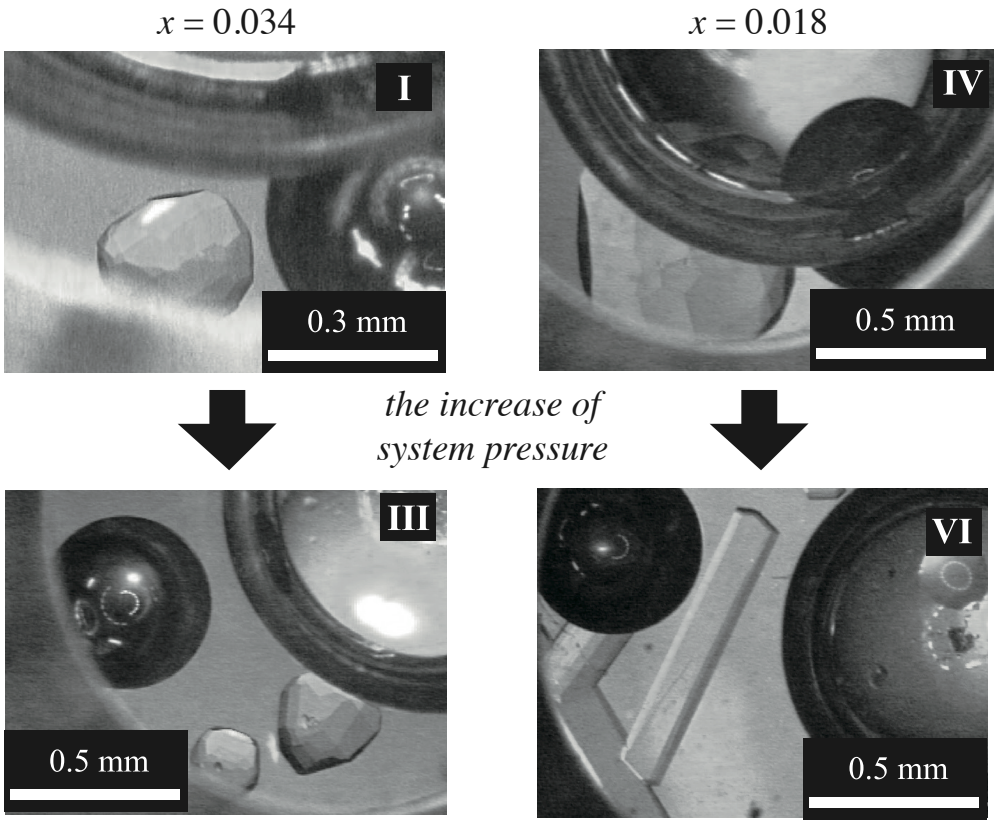

Fig. 4-5 Photos of single crystals for the H_2+TBAF semi-clathrate hydrate; (x = 0.034) p = 7.57 MPa, T = 301.28 K (I), p = 38.1 MPa, T = 303.49 K (III); (x = 0.018) p = 7.38 MPa, T = 299.15 K (IV), p = 34.7 MPa, T = 301.72 K (VI). Each label corresponds to that of **Fig. 4-3**. The ball that looks black is the ruby ball for the agitation in the high-pressure optical cell. The H_2 bubble is shown in the upper right in both pictures. All single crystals exist in the aqueous solution phase.

Combined with the results from phase behavior, Raman spectra of H_2, and appearance of crystal, only in the case of x = 0.018, it is suggested that the phase transition in the hydrate crystal occurred around 9 MPa and 299.3 K. The new structure is unclear because there is no direct evidence to specify structure. It is speculated that the new structure would be probably a tetragonal structure (TBAF·32.3H_2O), which can occupy much more H_2 than the cubic one (TBAF·28.6H_2O). As mentioned above, the tetragonal structure seems to be metastable for the simple TBAF hydrate, and it consists of 10 S-cages, 16 M-cages, and 4 L'-cages. Hence, the tetragonal structure has more S-cages in the unit-cell structure than the cubic one. As shown in **Fig. 4-3**, there is little change of Raman spectra derived from the TBAF molecule between cubic and new structures. This is why the cage size that entraps TBAF molecule would change little under the present experimental conditions.

4. 4. Conclusion

The thermodynamic stability and H_2 occupancy for the H_2+TBAF semi-clathrate hydrate system were investigated by phase equilibrium (pressure-temperature) measurements and Raman spectroscopic analyses at two mole fractions, x = 0.018 or 0.034, of TBAF aqueous solution. In the case of x = 0.034 (stoichiometric mole fraction for the cubic TBAF hydrate), the three-phase (hydrate + aqueous solution + gas) equilibrium curves of H_2+TBAF semi-clathrate hydrate lies at about 23 K higher temperature than that of H_2+THF mixed hydrate, while the storage amount of H_2 is smaller. In the case of x = 0.018 (lower than the stoichiometric mole fraction for the tetragonal TBAF hydrate), the Raman spectra and appearance of crystal obtained from the single crystal of H_2+TBAF semi-clathrate hydrates reveal that the structural transition from cubic structure to a new one occurs under the present experimental conditions. The new structure can store more H_2 molecules than the cubic ones. The stability boundary of H_2+TBAF semi-clathrate hydrate for x = 0.018 is shifted to slightly low-temperature or high-pressure side from that of x = 0.034.

Notation

a: lattice parameter [m]
p: pressure [Pa]
T: temperature [K]
x: mole fraction of TBAF in the aqueous solution [-]

References

[1] Hashimoto, S.; Murayama, S.; Sugahara, T.; Sato, H.; Ohgaki, K. "Thermodynamic and Raman Spectroscopic Studies on H_2 + Tetrahydrofuran + Water and H_2 + Tetra-*n*-butyl Ammonium Bromide + Water Mixtures Containing Gas Hydrates.", *Chemical Engineering Science*, **61**, 7884-7888 (2006).

[2] Chapoy, A.; Anderson, R.; Tohidi, B. "Low-pressure Molecular Hydrogen Storage in Semi-clathrate Hydrates of Quaternary Ammonium Compounds.", *Journal of the American Chemical Society*, **129**, 4, 746-747 (2007).

[3] Aladko, L. S.; Dyadin, Y. A.; Rodionova, T. V.; Terekhova, I. S. "Clathrate Hydrates of Tetrabutylammonium and Tetraisoamylammonium Halides.", *Journal of Structural Chemistry*, **43(6)**, 990-994 (2002).

[4] Shimada, W.; Ebinuma, T.; Oyama, H. "Separation of Gas Molecule Using Tetra-*n*-butyl Ammonium Bromide Semi-clathrate Hydrate Crystals.", *Japanese Journal of Applied Physics*, **42**, L129-L131 (2003).

[5] Shimada, W.; Shiro, M.; Kondo, H.; Takeya, S.; Oyama, H.; Ebinuma, T.; Narita, H. "Tetra-*n*-butylammonium Bromide-Water (1/38).", *Acta Crystallographica Section C*, **C61**, o65-o66 (2005).

[6] Oyama, H.; Shimada, W.; Ebinuma, T.; Kamata, Y.; Takeya, S.; Uchida, T.; Nagao, J.; Narita, H. "Phase Diagram, Latent Heat, and Specific Heat of TBAB Semiclathrate Hydrate Crystals." *Fluid Phase Equilibria*, **234**, 131-135 (2005).

[7] Hashimoto, S.; Sugahara, T.; Moritoki, M.; Sato, H.; Ohgaki, K. "Thermodynamic Stability of Hydrogen + Tetra-*n*-Butyl Ammonium Bromide Mixed Gas Hydrate in Nonstoichiometric Aqueous Solutions.", *Chemical Engineering Sci*ence, **63(4)**, 1092-1097 (2008).

[8] Dyadin, Y. A.; Telekhova, I. S.; Polyanskaya, T. M.; Aladko, L. S. "Clathrate Hydrates of Tetrabutylammonium Fluoride and Oxalate.", *Journal of Structural Chemistry*, **17**, 566-571 (1977).

[9] Komarov, V. Y.; Radionova, T. V.; Terekhova, I. S.; Kuratieva, N. V. "The cubic superstructure-I of tetra butyl ammonium fluoride $(C_4H_9)_4NF29.7H_2O$ clathrate hydrate.", *Journal of Inclusion Phenomena and Macro cyclic Chemistry*, **59**, 11-15 (2007).

Chapter 5

Thermodynamic Properties of Hydrogen + Trimethylamine Semi-clathrate Hydrate

Abstract

The thermodynamic stability and hydrogen occupancy for the hydrogen + trimethylamine mixed semi-clathrate hydrate system were investigated by means of phase equilibrium (pressure-temperature) measurements and Raman spectroscopic analyses. The hydrogen molecule gradually advanced to occupy the empty small cage of trimethylamine hydrate in proportion to pressure increase. Almost all small cages were filled up with the hydrogen molecules at about 80 MPa. Isothermal Raman spectroscopic analysis showed that the absorption-rate of hydrogen to the pre-treated trimethylamine hydrate was comparable to those of tetrahydrofuran hydrate. Only one hydrogen molecule was enclosed with one small cage at the equilibrium state in pre-treated trimethylamine hydrate.

Keywords: Semi-clathrate hydrate, Phase equilibria, Stability, Gas storage, Solutions, Gases

5. 1. Introduction

In the H_2 + second component (additive) mixed hydrate systems, the cage occupancy of H_2 is independent of the concentration of additive in the aqueous solution. The additive fully occupies the large cages, where as the small cages are occupied selectively with H_2 [1, 2]. In addition, as an interesting technique for the H_2 storage method using mixed hydrates, it has been reported that the H_2 storage and release for THF hydrate can be performed reversibly by pressure swing without destroying hydrate cages [3-5]. It is necessary to search a suitable additive that is able to satisfy the following requests simultaneously: a high stability, a high H_2 storage density, and a reversible storage and release of H_2 for an additive hydrate.

Trimethylamine (hereafter, TMA) has been adopted as a new candidate of additives in the present study. TMA semi-clathrate hydrate is stable under milder conditions than that of THF hydrate [6, 7]. There are various reports about the mole ratio of TMA to H_2O for simple TMA hydrate: TMA·$10H_2O$ [7], TMA·$10.25H_2O$ [8], and TMA·$11H_2O$ [6]. Panke [8] has reported the crystal structure of TMA hydrate. The unit-cell of TMA hydrate has hexagonal structure which is composed of three S-cages, two L'-cages, and a connected cavity of two M-cages (hereafter, connected M-cage). Two TMA molecules occupy the connected M-cage and one occupies L'-cage completely, while the S-cage of TMA hydrate remains empty. The hydrogen bond specifically exists between the N atom of TMA molecule and the H atom of water molecules constructing hydrate cages. That is, these hydrogen bonds may destroy partially the water framework of TMA hydrate and distort the connected M- and L'-cages. One of the reasons for the adoption of TMA in the present study is to investigate whether H_2 can be encaged with TMA molecule in the distorted large cages occupied by TMA molecule.

In Chapter 5, thermodynamic stability of the H_2+TMA mixed semi-clathrate hydrate has been measured. In addition, the cage occupancy of H_2 in the mixed semi-clathrate hydrate has been investigated along the thermodynamic stability boundary by means of *in situ* Raman spectroscopy. Finally, the H_2 storage process of TMA hydrate by pressurization has been evaluated by means of *in situ* Raman spectroscopy under the isothermal conditions.

5. 2. Experimental

5. 2. 1. Apparatus

All apparatus are the same ones and details are shown in Chapters 1 and 2.

5. 2. 2. Procedures

Experimental procedures of Raman spectroscopic analyses are same shown in Chapter 3, except for the mole fraction of TMA aqueous solution, which is 0.047 or 0.083. The latter one is the stoichiometric concentration of TMA semi-clathrate hydrate.

In the isothermal measurement, the TMA aqueous solution prepared at the stoichiometric composition was introduced into the evacuated high-pressure optical cell. Then the contents were pressurized up to a desired pressure by supplying H_2. They were supercooled and agitated with an enclosed ruby ball to prepare the H_2+TMA mixed semi-clathrate hydrate. They were annealed at 278.15 K that is slightly lower than the equilibrium temperature of TMA hydrate at atmospheric pressure for at least a day, in order to achieve the two-phase equilibrium (H_2 fluid and hydrate phases). The TMA hydrate was prepared through the pre-treatment procedure where the H_2 was released by depressurization from the H_2+TMA mixed semi-clathrate hydrate. The pre-treatment is quite important to obtain good reproducible results. Although the reason is still unclear now, the author speculates that the interfacial film of primary particle would play a role as a barrier against H_2 diffusion from outside. To consider the H_2 diffusivity, isothermal Raman measurement in the hydrate phase was performed at various neighbor positions on the fluid phase, which were ~750 μm away from the fluid-hydrate interface.

5. 2. 3. Materials

Research grade H_2 (mole fraction purity: 0.999999) was obtained from the Neriki Gas Co., Ltd. The maximum impurity was 0.2 ppm of nitrogen. Research grade TMA (*ca*. 28 mass% aqueous solution) was obtained from the Tokyo Chemical Industry, Co., Ltd. The distilled water was obtained from the Wako Pure Chemicals Industries, Ltd. All of them were used without further purifications.

5. 3. Results and Discussion

5. 3. 1. Thermodynamic Property

Phase equilibrium (pressure-temperature) relations at two TMA concentrations (x = 0.047 or 0.083) for the H_2+TMA mixed semi-clathrate hydrate system are summarized in **Table 5-1** and shown in **Fig. 5-1**. The latter concentration is close to the stoichiometric composition of hexagonal TMA hydrate. Each three-phase equilibrium pressure increases monotonically from 0.1 to 170 MPa as the temperature increases. The three-phase equilibrium curve obtained at x = 0.047 is shifted to the lower-temperature side than that of x = 0.083. These phase behaviors are similar to those of H_2 + other assistant-additive mixed hydrate systems obtained in our previous studies [9].

Figure 5-2 shows a single crystal of H_2+TMA mixed semi-clathrate hydrate with x = 0.083, 163 MPa and 300.3 K. **Figure 5-3** shows the characteristic Raman peaks derived from TMA in the H_2+TMA mixed semi-clathrate hydrate. **Figure 5-3(a)** includes the four peaks corresponding to the H_2

Table 5-1 Experimental dissociation conditions of H_2+TMA semi-clathrate hydrate at the TMA mole fraction of 0.047 and 0.083.

	***T* / K**	***p* / MPa**		***T* / K**	***p* / MPa**
x = 0.083	278.88	0.31	x = 0.047	275.76	0.33
	279.10	1.03		275.94	0.98
	279.42	1.95		276.29	2.01
	279.70	2.94		276.63	2.99
	279.99	3.94		276.88	3.92
	280.26	4.88		277.21	4.94
	280.56	5.87		277.62	5.97
	280.81	6.89		277.91	6.93
	281.07	7.84		278.11	7.83
	281.36	8.86		278.30	8.58
	281.57	9.80		290.89	78.3
	284.04	19.5		294.00	107.8
	288.47	44.7		298.01	156.9
	291.67	67.2			
	294.62	101.7			
	298.10	136.7			
	300.74	172.8			

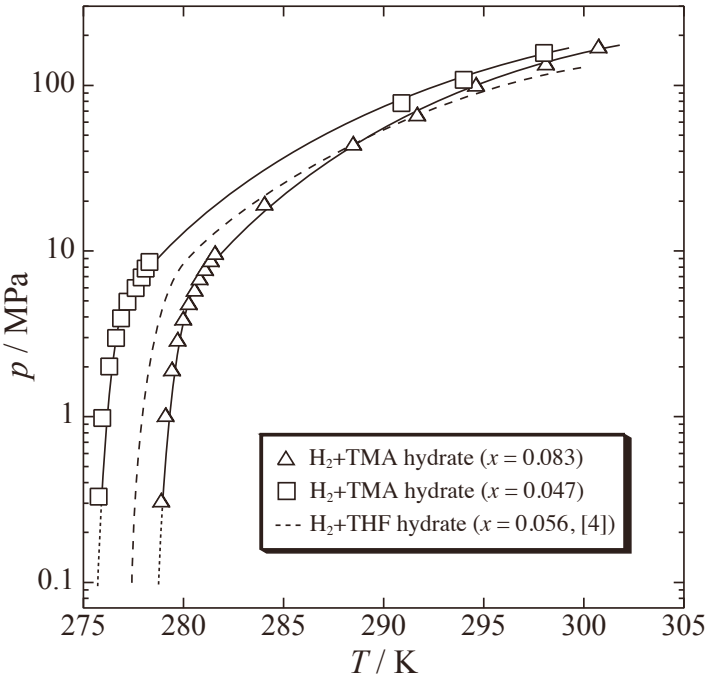

Fig. 5-1 Three-phase equilibrium curves of the H_2+TMA mixed semi-clathrate hydrate. The solid lines stand for the smoothed values.

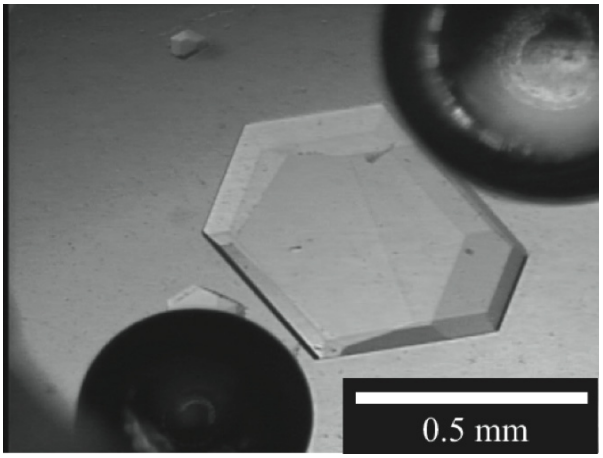

Fig. 5-2 The micrograph of single crystal in the H_2+TMA mixed semi-clathrate hydrate system (x = 0.083, p = 163 MPa, T = 300.03 K). The ruby sphere looks black is inserted in the high-pressure optical cell. The H_2 bubbles is shown in the upper right. The single crystal exists in the aqueous phase.

rotation, which are detected at 354, 588, 816, and 1036 cm^{-1}. The positions of these peaks for the H_2 rotation are coincident with our previous reports [1, 9]. **Figure 5-3(b)** includes the broad peak corresponding to the O–H vibration of host water lattice. There is no remarkable change of Raman spectra corresponding to TMA under the various TMA concentration, pressure and temperature conditions for the H_2+TMA mixed semi-clathrate hydrate. That is, the structural transition of H_2+TMA semi-clathrate hydrate may not occur unlike the H_2+TBAB semi-clathrate hydrate system [2].

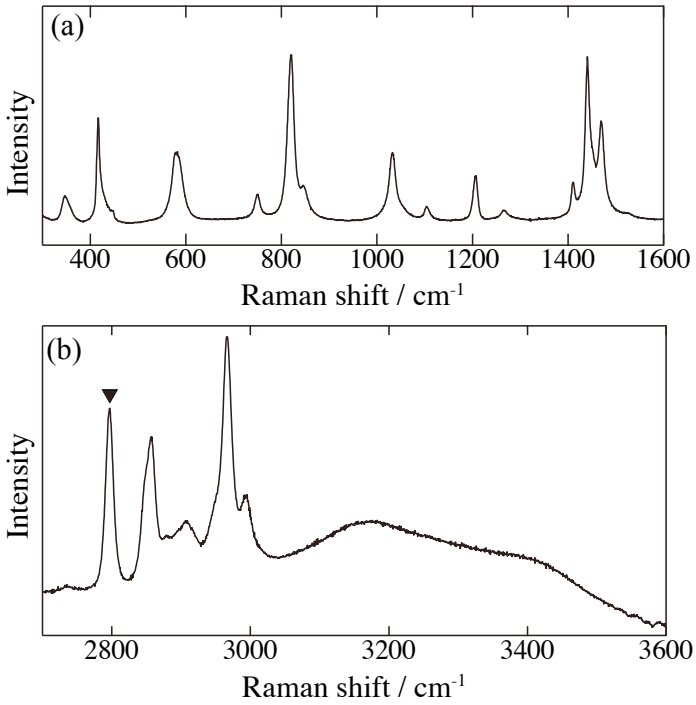

Fig. 5-3 Typical Raman spectra derived from TMA in the hydrate phase for the H_2+TMA mixed semi-clathrate hydrate system in the low (a) and high (b) wavenumber ranges. Closed inverted-triangle represents the peak for the normalization of H_2 vibration peak. The peaks detected around 420 and 750 cm^{-1} are corresponding to the upper sapphire window of high-pressure optical cell.

The peak corresponding to H_2 vibration in the H_2+TMA mixed semi-clathrate hydrate with x = 0.083 and 0.047 is shown in **Figs. 5-4** and **5-5**, respectively. All spectra in **Figs. 5-4** and **5-5** are normalized with the peak around 2800 cm^{-1} (closed inverted triangle in **Fig. 5-3**) derived from TMA. As shown in **Figs. 5-4** and **5-5,** a single peak corresponding to the H–H stretching vibration is detected at 4132 cm^{-1} in the hydrate phase. The position and shape of the peak derived from H_2 obtained in the present study agree well with those of other mixed-H_2 hydrates [1, 2, 9]. The normalized peak intensity of H_2 vibration increases successively with the increase of system pressure. This indicates that the storage amount of H_2 increases as pressure rises.

Figure 5-6 shows the pressure dependence of normalized peak area of H_2 vibration. The storage amount of H_2 reaches plateau at ~80 MPa. That is, the H_2 molecule gradually occupies the empty S-cage of TMA hydrate with the pressure increased and then the S-cages are filled up with H_2 almost completely at ~80 MPa which is coincident with that of H_2+THF hydrate. Even at pressures higher than 80 MPa, neither the L'-cage nor the connected M-cage is occupied by H_2. Moreover, no multi-occupancy of H_2 is observed in the S-cage. These results show that the cage occupancy of H_2 in the H_2+TMA mixed semi-clathrate hydrate depends on neither the TMA mole fraction in the mother solution nor the system pressure. Whereas the H_2 selectively occupies the empty S-cages of TMA hydrate, the TMA molecule occupies the other cages completely.

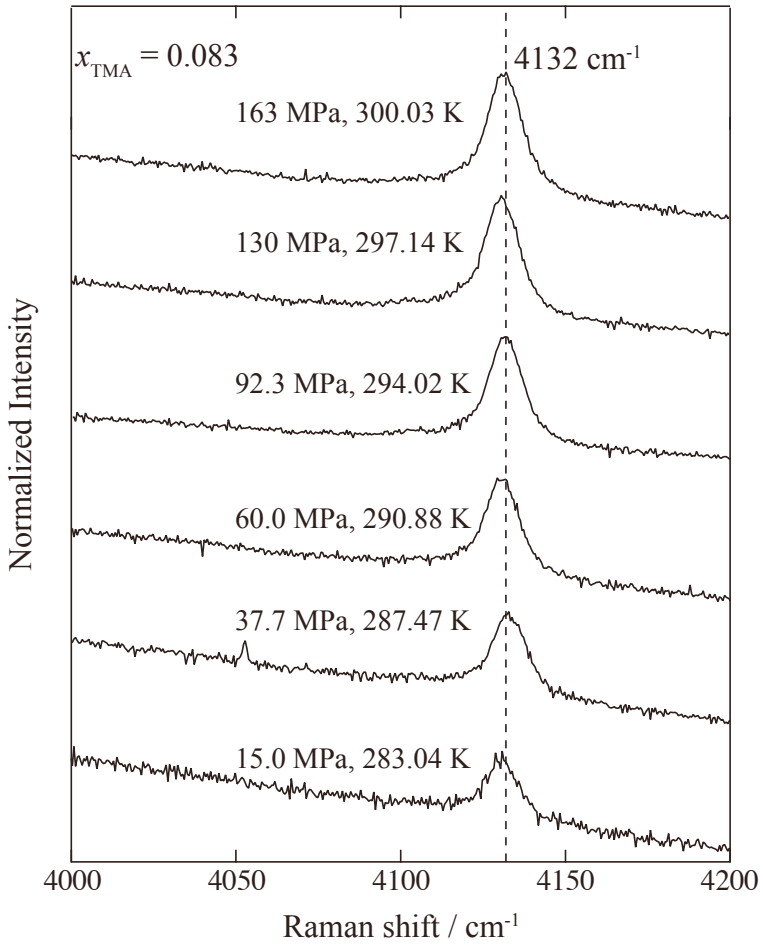

Fig. 5-4 Raman spectra corresponding to the intramolecular vibration of H_2 in the H_2+TMA mixed semi-clathrate hydrate prepared along the phase-equilibrium boundary at x = 0.083.

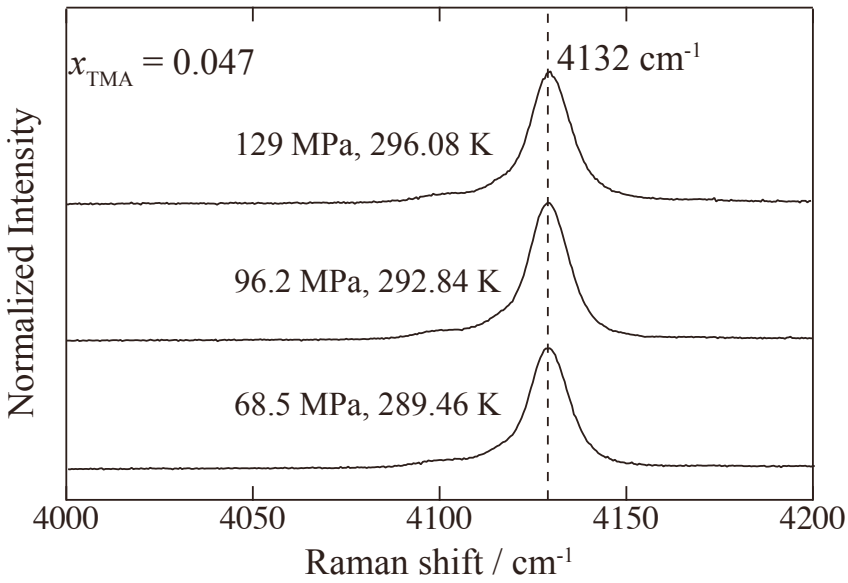

Fig. 5-5 Raman spectra corresponding to the intramolecular vibration of H_2 in the H_2+TMA mixed semi-clathrate hydrate prepared along the phase-equilibrium boundary at x = 0.047.

From the isothermal Raman measurements for the H_2 absorption to pre-treated TMA hydrate (hereafter, TMA hydrate) at 278.15 K, the time variation of H_2 vibration peak for the TMA hydrate at 61.5 MPa is shown in **Fig. 5-7**. These peaks are obtained under the isothermal conditions. As discussed previously, they are normalized by use of the peak derived from TMA. The measuring point is ~750 μm away from the fluid-solid (hydrate) interface, which is always the same. In addition, we have confirmed almost the same results at a couple of similar points of 750 μm away from the interface. The peak intensity reaches plateau within 1 day, which is comparable with the H_2 absorption rate of THF hydrate [4]. In addition, as shown in **Fig. 5-6** (closed triangle-key), the storage amount of H_2 in the semi-clathrate hydrate is comparable with the H_2 amount of the H_2+TMA mixed semi-clathrate hydrate prepared from H_2 and TMA aqueous solution similar pressure which is obtained under the three-phase equilibrium condition.

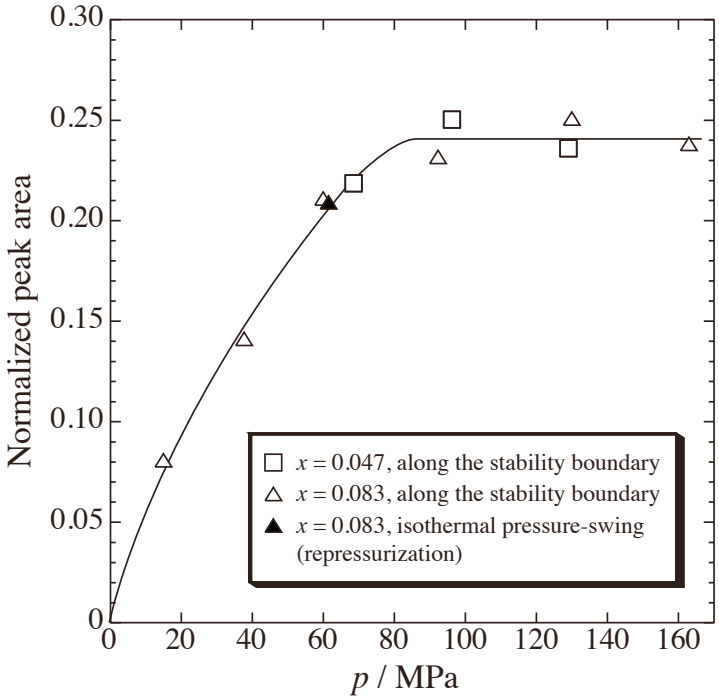

Fig. 5-6 The pressure dependence of the normalized peak area (H_2 vibration / a peak derived from TMA). The solid line stands for the smoothed values.

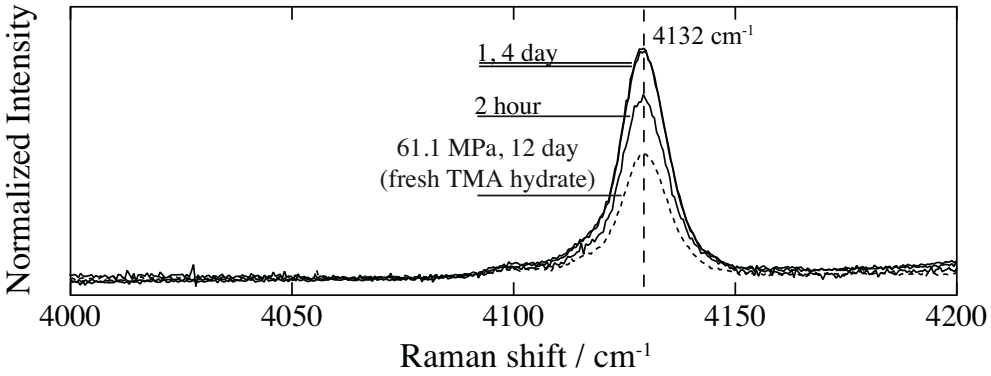

Fig. 5-7 The H_2 vibration peak obtained from the isothermal experiments for the TMA hydrate at 61.5 MPa.

2. 4. Conclusion

The three-phase equilibrium relations and cage occupancy of H_2 for the H_2+TMA mixed semi-clathrate hydrate system were investigated by means of the phase equilibrium (pressure-temperature) measurements and Raman spectroscopic analysis. Regardless of the TMA concentration, the structure and H_2 occupancy of H_2+TMA hydrate do not change under the present experimental conditions up to 170 MPa. The H_2 molecule gradually advances to occupy the empty S-cages of TMA hydrate as pressure rises, and then the S-cages are filled up with H_2 almost completely at about 80 MPa. The H_2-saturated pressure and H_2 absorption-rate of TMA hydrate is comparable to the case of THF hydrate.

Notation

p: pressure [Pa]
T: temperature [K]
x: mole fraction of TMA in the aqueous solution [-]

References

[1] Hashimoto, S.; Sugahara, T.; Sato, H.; Ohgaki, K. "Thermodynamic Stability of H_2 + Tetrahydrofuran Mixed Gas Hydrate in Nonstoichiometric Aqueous Solutions.", *Journal of Chemical & Engineering Data*, **52**, 517-520 (2007).

[2] Hashimoto, S.; Sugahara, T.; Moritoki, M.; Sato, H.; Ohgaki, K. "Thermodynamic Stability of Hydrogen + Tetra-*n*-Butyl Ammonium Bromide Mixed Gas Hydrate in Nonstoichiometric Aqueous Solutions.", *Chemical Engineering Sci*ence, **63(4)**, 1092-1097 (2008).

[3] Strobel, T. A.; Taylor, C. J.; Hester, K. C.; Dec, S. F.; Koh, C. A.; Miller, K. T.; Sloan, E. D., Jr. "Molecular Hydrogen Storage in Binary THF-H2 Clathrate Hydrates.", *Journal of Physical Chemistry B*, **110**, 17121-17125 (2006).

[4] Ogata, K.; Hashimoto, S.; Sugahara, T.; Moritoki, M.; Sato, H.; Ohgaki, K. "Storage Capacity of Hydrogen in Tetrahydrofuran Hydrate.", *Chemical Engineering Science*, **63(23)**, 5789-5794 (2008).

[5] Nagai, Y.; Yoshioka, H.; Ota, M.; Sato, Y.; Inomata, H.; Smith, R. L., Jr.; Peters, C. J. "Binary Hydrogen-Tetrahydrofuran Clathrate Hydrate Formation Kinetics and Models.", *AIChE Journal*, **54(11)**, 3007-3016 (2008).

[6] Pickering, S. U. "The Hydrate Theory of Solutions. Some Compounds of the Alkyl-amines and Ammonia with Water.", *Journal of the Chemical Society*, *Transactions*, **63**, 141-195 (1893).

[7] Somerville, W. C. "An Investigation of the Degrees of Hydration of the Alkyl Amines in Aqueous Solution.", *Journal of Physical Chemistry*, **35**, 2412-2433 (1931).

[8] Panke, D. "Polyhedral Clathrate Hydrates. XV. The Structure of $4(CH_3)_3N{\cdot}41H_2O$.", The *Journal of Chemical Physics*, **48**, 2990-2996 (1967).

[9] Hashimoto, S.; Murayama, S.; Sugahara, T.; Sato, H.; Ohgaki, K. "Thermodynamic and Raman Spectroscopic Studies on H_2 + Tetrahydrofuran + Water and H_2 + Tetra-*n*-butyl Ammonium Bromide + Water Mixtures Containing Gas Hydrates.", *Chemical Engineering Science*, **61**, 7884-7888 (2006).

Chapter 6

Thermodynamic Properties of Hydrogen + Tetra-*n*-butyl Phosphonium Bromide Semi-clathrate Hydrate

Abstract

Three-phase equilibrium (pressure-temperature) relation of hydrate + aqueous + fluid phases for the hydrogen (H_2) + tetra-*n*-butyl phosphonium bromide (TBPB) + water ternary system was investigated in a temperature range of 281.90-295.94 K and a pressure range up to 170 MPa. The behavior of the three-phase coexisting curve indicates no structural transition in the present experimental region. The Raman spectra obtained in the H_2+TBPB mixed semi-clathrate hydrate crystal reveal that H_2 molecule occupies only small cage compartmentally and the TBPB molecule is encaged with a set of other large cages.

Keywords: Gas hydrate, Phase equilibria, Raman spectroscopy, Stability, Energy, Solutions

6. 1. Introduction

Tetra-*n*-butyl phosphonium bromide (hereafter, TBPB) has been regarded as a semi-clathrate hydrate former. TBPB semi-clathrate hydrates have at least four lattice-cells with different mole ratios of TBPB to H_2O. They have been reported 32 and 37.5 as congruent melting compositions, 24 and 26 as incongruent melting compositions [1], while all of unit-cells are still unclear. The three-phase equilibrium relation of H_2+TBPB semi-clathrate system with the mole ratio of TBPB to H_2O of 32 has been already reported [2]. The TBPB semi-clathrate hydrate with the mole ratio of 37.5 (the concentration in aqueous solution, x = 0.026) is stable up to the highest temperature of 282.05 K at atmospheric pressure. The mole ratio (37.5) of the most stable TBPB semi-clathrate hydrate is larger than those of TBAB (26) and TBAF (28.6) semi-clathrate hydrates, which has the advantage of less additive.

In the Chapter 6, the thermodynamic stability of H_2+TBPB semi-clathrate hydrates with mole ratio of 37.5 has been investigated at a pressure up to 170 MPa. The small-cage occupancy of H_2 in the mixed semi-clathrate hydrate was discussed based on the Raman spectra obtained under three-phase equilibrium conditions.

6. 2. Experimental

6. 2. 1. Apparatus

All apparatus are the same ones and details are shown in Chapters 1 and 2.

6. 2. 2. Procedures

Experimental procedures are same shown in Chapter 3, except for the mole fraction of TBPB aqueous solution, which is 0.026.

6. 2. 3. Materials

Research grade H_2 (mole fraction purity: 0.999999) was obtained from the Neriki Gas Co., Ltd. The maximum impurity was 0.2 ppm of nitrogen. Research grade TBPB (mole fraction purity: 0.997) and the distilled water were obtained from the Wako Pure Chemicals Industries, Ltd. All of them were used without further purifications.

6. 3. Results and Discussion

The three-phase equilibrium (*p*-*T*) relation for the H_2+TBPB semi-clathrate hydrate are summarized in **Table 6-1** and shown in **Fig. 6-1**. The stability boundary curve of H_2+TBPB semi-clathrate hydrate originates at the vicinity of atmospheric equilibrium temperature (282.05 K, [1]) of simple TBPB semi-clathrate hydrate with $x = 0.026$, and vertically rises up in the pressure up to ~1 MPa. The equilibrium pressure increases continuously with the temperature increasing. Since this curve continues smoothly, no structural transition would occur under the present experimental conditions.

The Raman spectra for the H_2+TBPB semi-clathrate hydrate under the three-phase equilibrium conditions are shown in **Fig. 6-2**. The peaks derived from sapphire window are detected around 751 cm^{-1} (displayed by the symbol of *). The characteristic Raman peaks derived from TBPB molecule are detected around 600-1500 cm^{-1} and 2700-3000 cm^{-1} in both hydrate and aqueous phases. **Figure 6-2** includes the broad peak (3100-3400 cm^{-1}) of the O–H vibration of host water for the H_2+TBPB semi-clathrate hydrate. The peak of the H_2 stretching vibration (4131 cm^{-1}) is normalized by use of one of the Raman peaks derived from TBPB (displayed by the symbol of ▼). The position and shape of the peak derived from H_2 obtained in the present study are consistent with those of H_2+TBAB semi-clathrate hydrate [3, 4]. Although the peak position is stationary, normalized peak area of H_2 vibration increases with the pressure increasing, which means the amount of entrapped H_2 molecules increases. This indicates that H_2 selectively occupies empty small- (or similar size) cage of hydrates are almost independent of pressure. No structural transition appears under present experimental conditions.

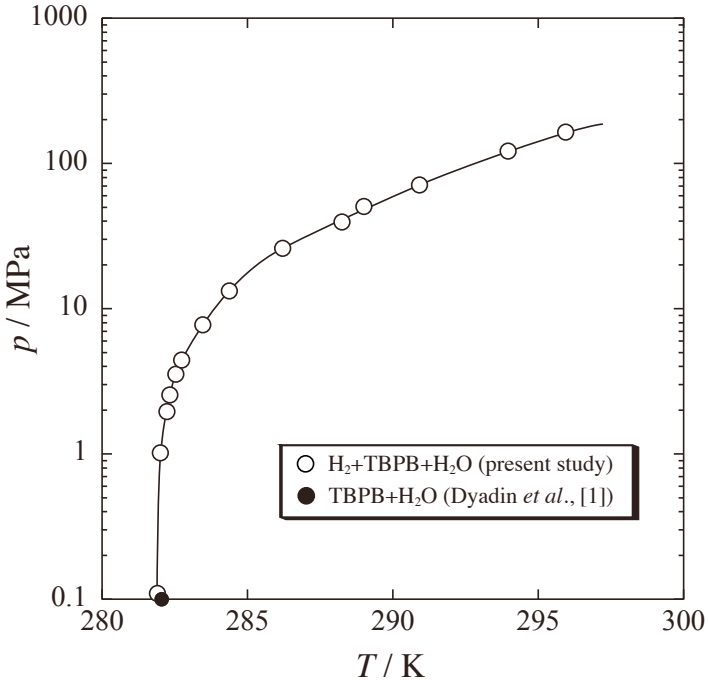

Fig. 6-1 Three-phase equilibrium curve of the H_2+TBPB semi-clathrate hydrate ($x = 0.026$).

Table 6-1 Three-phase equilibrium relation of H_2+TBPB semi-clathrate hydrate (x = 0.026).

***T* / K**	***p* / MPa**	***T* / K**	***p* / MPa**
281.90	0.11	284.37	13.3
282.00	1.02	286.21	26.1
282.23	1.96	288.25	39.7
282.33	2.55	289.00	50.7
282.53	3.55	290.91	71.3
282.73	4.44	293.96	121.7
283.46	7.77	295.94	164.6

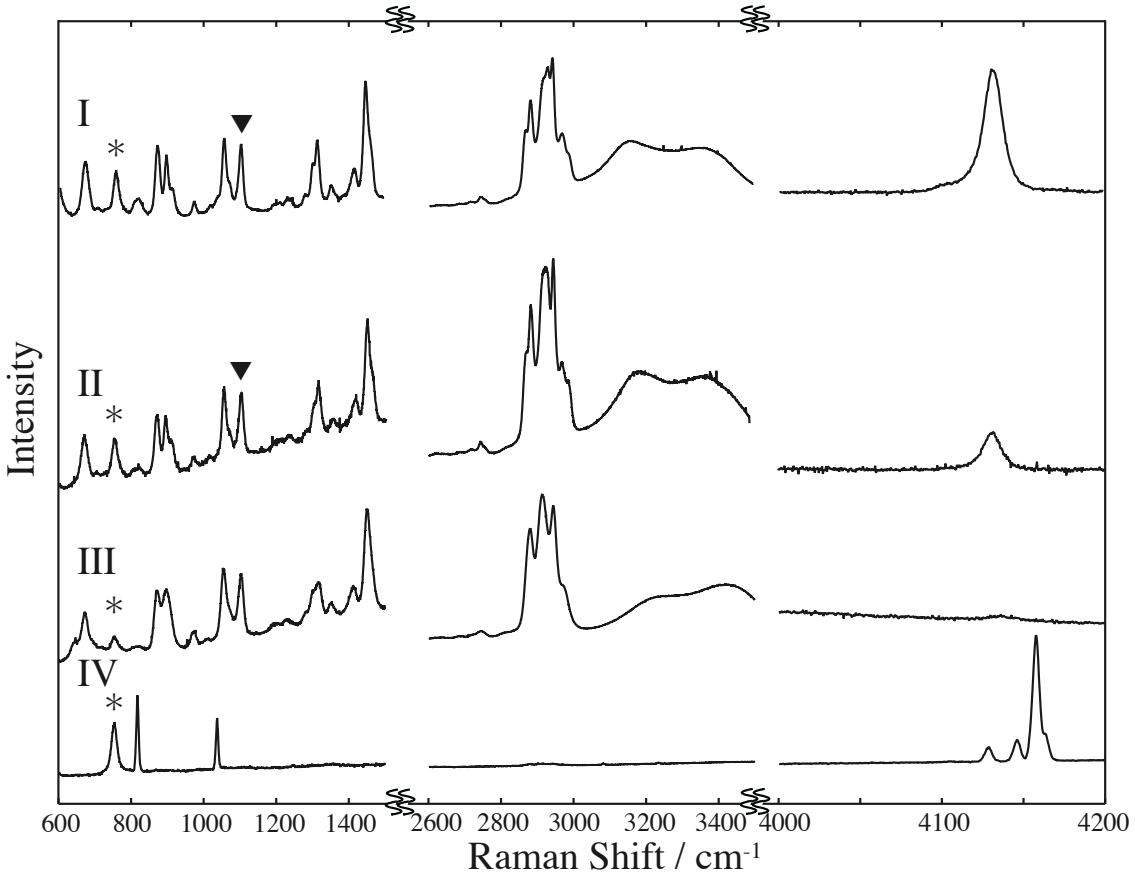

Fig. 6-2 Raman spectra originated in TBPB, H_2 and host lattice of water in hydrate (I-II), aqueous (III) and fluid (IV) phases (x = 0.026); I: 295.48 K, 181.7 MPa; II-IV: 283.19K, 11.8 MPa.

The Raman peaks derived from TBPB in semi-clathrates are almost independent of pressure. No structural transition appears under present experimental conditions.

6. 4. Conclusion

The stability boundary curve of H_2+TBPB semi-clathrate hydrate converges at the vicinity of the equilibrium temperature (281.90 K) of simple TBPB semi-clathrate hydrate. The results reveal no structural phase transition in the H_2+TBPB semi-clathrate hydrate with x = 0.026. The small-cage occupancy of H_2 depends on the pressure and no H_2 molecule occupies any other larger cages at a pressure up to 170 MPa.

Notation

p: pressure [Pa]
T: temperature [K]
x: mole fraction of TBPB in the aqueous solution [-]

References

[1] Dyadin, Yu. A.; Zelenina, L. S.; Zelenin, Yu. M.; Yakovlev, I. I.; "Izvestiya Sibirskogo Otdeleniya Akademii Nauk SSSR.", *Seriya Khimicheskikh Nauk*, **4**, 30-33 (1973).

[2] Deschamps, J.; Dalmazzone, D. "Hydrogen Storage in Semiclathrate Hydrates of Tetrabutyl Ammonium Chloride and Tetrabutyl Phosphonium Bromide.", *Journal of Chemical & Engineering Data*, **55**, 3395-3399 (2010).

[3] Hashimoto, S.; Murayama, S.; Sugahara, T.; Sato, H.; Ohgaki, K. "Thermodynamic and Raman Spectroscopic Studies on H_2 + Tetrahydrofuran + Water and H_2 + Tetra-*n*-butyl Ammonium Bromide + Water Mixtures Containing Gas Hydrates.", *Chemical Engineering Science*, **61**, 7884-7888 (2006).

[4] Hashimoto, S.; Sugahara, T.; Moritoki, M.; Sato, H.; Ohgaki, K. "Thermodynamic Stability of Hydrogen + Tetra-*n*-Butyl Ammonium Bromide Mixed Gas Hydrate in Nonstoichiometric Aqueous Solutions.", *Chemical Engineering Sci*ence, **63(4)**, 1092-1097 (2008).

GENERAL CONCLUSION

In this thesis, the cage occupancy of H_2 in H_2+various second components mixed hydrates has been studied mainly by means of phase equilibrium measurement, Raman spectroscopic analysis, and *p-V-T* measurement. The fundamental findings obtained in the present study are quite important to develop the future technologies, that is, the utilization of gas hydrates as gas storage media, as well as to understand the characters of mixed hydrates. The achievements in my studies are divided into two parts according to the hydrate structures; the former part (Part A) involves in traditional type of clathrate hydrates, especially s-II clathrate hydrates, and the latter one (Part B) contains the information on semi-clathrate hydrates.

PART A: CLATHRATE HYDRATE SYSTEMS

In this part, the s-II hydrates containing Ar, and five-membered ring molecules such as THT, furan, and *c*-C_5H_{10} were focused. Ar molecules occupy both S- and L-cages, and five-membered ring molecules are entrapped only in L-cage.

Firstly, the cage occupancies of H_2 in both simple H_2 hydrate and H_2+Ar mixed-gas hydrate were investigated under the three-phase equilibrium conditions by Raman spectroscopic analysis. In both hydrate systems, three broadened peaks were detected around ~4140 cm^{-1}. These peaks correspond to the intramolecular H–H stretching vibration mode of H_2 in S- and L-cages. In addition, Raman spectra for the H_2+Ar mixed-gas hydrate were measured at 77 K. Multiple peaks of H_2 vibrons were detected between 4120 and 4160 cm^{-1}, and these peaks can be deconvoluted into eight peaks, which are identified as one ortho- (or para-) H_2 molecule in S-cage, and two, three, or four ortho- (or para-) ones in the L-cage. In the H_2+Ar mixed-gas hydrates, L-cage is occupied by a cluster of two, three, or four H_2 molecules similar as in the case with simple H_2 hydrate, while the pressure dependence of L-cage occupancy of H_2 differs from that of simple H_2 hydrates. These indicate that four H_2 clusters occupy the L-cages competitively with Ar in the equilibrium pressure region higher than ~25 MPa at an ambient temperature.

Secondly, the cage occupancy of H_2 in H_2+THT, furan and *c*-C_5H_{10} mixed hydrates was investigated under the isothermal conditions (THT and furan hydrate systems at ~275.1 K, and *c*-C_5H_{10} hydrate system at ~277.1 K) by *p-V-T* measurement. The pressure dependence of H_2 occupancy in the systems exhibited the similar behavior. Additionally, it is inferred that the occupancy would reach plateau at ~80 MPa. Analogizing with THF hydrate, H_2 molecules are singly entrapped only in S-cages, while five-membered ring molecules are only in L-cages. The initial absorption rates of H_2 in THT, furan, and *c*-C_5H_{10} hydrates become large with pressure increasing, and they are larger than that of THF hydrate, while H_2 storage capacities are nearly equivalent. It is speculated that this discrepancy would attribute to the expansion or distortion of hydrate cages, and physical and chemical properties of additives such as solubility.

PART B: SEMI-CLATHRATE HYDRATE SYSTEMS

In this part, the cage occupancies of H_2 in various semi-clathrate hydrates containing TBAB, TBAF, TMA, and TBPB were investigated by Raman spectroscopic analysis and phase equilibrium measurement. The Raman spectra corresponding to the second components did not change with pressure increasing in each semi-clathrate hydrate with the stoichiometric composition. Moreover, three-phase equilibrium curves exhibited no characteristic behavior like structural transition. On the other hand, in TBAB and TBAF semi-clathrate hydrates with a composition lower than the stoichiometric one, the

gradient of three-phase equilibrium curve (d*p*/d*T*) suddenly diminishes at ~95 MPa and ~9 MPa, respectively. In addition, the Raman spectra corresponding to the TBAB molecule changed into another shape under the same conditions, while those of TBAF molecule invoked no change. These facts reveal that the structural transition resulted from the increase of H_2 pressure. The new structure should contain more small cages.

The Raman peaks corresponding to the intramolecular H–H stretching vibration of H_2 became intense with pressure increasing in the semi-clathrate hydrate systems. In the TMA hydrate system, the intensity of these peaks reached plateau at ~80 MPa. This tendency resembles the case of the five-membered ring molecules hydrate systems as already mentioned above. While, these intensities in TBAB, TBAF, and TBPB semi-clathrate hydrate systems were not saturated up to 200 MPa, regardless of the preparation methods of H_2+additive mixed hydrates. This discrepancy is quite intriguing, because the semi-clathrate hydrates would contain S- (or similar size) cages and H_2 molecules could be entrapped in only these cages selectively, depending on the circumambient pressure. It is speculated the main factor would be that the quaternary ammonium / phosphonium salt molecules exist at ionized state in hydrate, and this might interrupt the diffusion of H_2.

Foresight into the Future Studies

In this thesis, I made great efforts to clarify the H_2 occupancies (H_2 storage abilities) in various H_2+additive mixed hydrates. The H_2 occupancy and lattice structure have been investigated by means of Raman spectroscopy, which is the indirect method. I have tried neutron and X-ray diffraction measurements, but there were some difficulties in sample preparation for the measurements with a high degree of accuracy. Additionally, the legal hurdle is prevented from utilizing the high-pressure facilities for the *in situ* observation.

In another instance, tuning effect is quite curious phenomenon as already mentioned in GENERAL INTRODUCTION. Utilizing this technique might be able to achieve that a number of H_2 could intrude into large cages of some semi-clathrate hydrates alternated with additive. That is, a new semi-clathrate hydrate system, which might have metastable structure, would have possibilities to become a candidate being superior in terms of H_2 storage abilities.

LIST OF PUBLICATIONS AND PRESENTATIONS

Publications

[1] Jun Sakamoto, Shunsuke Hashimoto, Takaaki Tsuda, Takeshi Sugahara, Yoshiro Inoue, Kazunari Ohgaki "Thermodynamic and Raman Spectroscopic Studies on Hydrogen+Tetra-*n*-butyl Ammonium Fluoride Semi-clathrate Hydrate.", *Chemical Engineering Science*, **63**, 5789-5794 (2008).

[2] Takaaki Tsuda, Kyohei Ogata, Shunsuke Hashimoto, Takeshi Sugahara, Kazunari Ohgaki "Storage Capacity of Hydrogen in Tetrahydrothiophene and Furan Clathrate Hydrates.", *Chemical Engineering Science*, **64**, 4150-4154 (2009).

[3] Shunsuke Hashimoto, Takaaki Tsuda, Kyohei Ogata, Takeshi Sugahara, Yoshiro Inoue, Kazunari Ohgaki "Thermodynamic Properties of Hydrogen + Tetra-*n*-Butyl Ammonium Semi-Clathrate Hydrate.", *Journal of Thermodynamics*, **2010**, 170819-1-170819-5 (2010).

[4] Kyohei Ogata, Takaaki Tsuda, Shingo Amano, Shunsuke Hashimoto, Takeshi Sugahara, Kazunari Ohgaki "Hydrogen Storage in Trimethylamine Hydrate: Thermodynamic Stability and Hydrogen Storage Capacity of Hydrogen + Trimethylamine Mixed Semi-Clathrate Hydrate.", *Chemical Engineering Science*, **65**, 1616-1620 (2010).

[5] Shingo Amano, Takaaki Tsuda, Shunsuke Hashimoto, Takeshi Sugahara, Kazunari Ohgaki "Competitive Cage-occupancy of Hydrogen and Argon in Structure-II Hydrates.", *Fluid Phase Equilibria*, **298**, 113-116 (2010).

[6] Takaaki Tsuda, Shunsuke Hashimoto, Takeshi Sugahara, Kazunari Ohgaki "Effect of Cyclopentane on Small-cage Occupancy of Hydrogen in Clathrate Hydrates.", *Physics and Chemistry of Ice*, **2010**, 277-281 (2011).

[7] Yuuya Fujisawa, Takaaki Tsuda, Shunsuke Hashimoto, Takeshi Sugahara, Kazunari Ohgaki "Thermodynamic Stability of Hydrogen + Tetra-*n*-butyl Phosphonium Bromide Mixed Semi-clathrate Hydrate.", *Chemical Engineering Science*, **68**, 660-662 (2012).

Other

[8] Takaaki Tsuda, Kyohei Ogata, Shunsuke Hashimoto, Takeshi Sugahara, Hiroshi Sato, Kazunari Ohgaki "Storage Capacity of Hydrogen in Gas Hydrates.", *Journal of Physics: Conference Series*, **215**, 012061-1-012061-5 (2010).

Presentations (International Conferences)

[1] Shunsuke Hashimoto, Jun Sakamoto, Kyohei Ogata, Takaaki Tsuda, Takeshi Sugahara, Yoshiro Inoue, Kazunari Ohgaki "The Potentiality of Clathrate Hydrates as a Hydrogen Storage Material.", *The 2nd SSCCI/SCEJ (Kansai-Branch) Joint International Conference on Chemical Engineering*, Shanghai, November (2008).

[2] Takaaki Tsuda, Kyohei Ogata, Shunsuke Hashimoto, Takeshi Sugahara, Hiroshi Sato, Kazunari Ohgaki "Storage Capacity of Hydrogen in Gas Hydrates.", *Joint AIRAPT-22 & HPCJ-50 International Conference on "High Pressure Science and Technology"*, Tokyo, July (2009).

[3] Takaaki Tsuda, Shunsuke Hashimoto, Takeshi Sugahara, Kazunari Ohgaki "Effect of Cyclopentane on Cage Occupancy of Hydrogen in Clathrate Hydrates.", *12th International Conference on Physics and Chemistry of Ice (PCI2010)*, Sapporo, September (2010).

[4] Takeshi Sugahara, Pinnelli S. R. Prasad, Vahid Taghikhani, Takaaki Tsuda, Kazunari Ohgaki, E. Dendy Sloan, Carolyn A. Koh, Amadeu K. Sum "Molecular Storage of Hydrogen in Simple and Binary Clathrate Hydrates.", *7th International Conference on Gas Hydrates (ICGH7)*, Edinburgh, July (2011).

[5] Takaaki Tsuda, Shingo Amano, Yuuya Fujisawa, Shunsuke Hashimoto, Takeshi Sugahara, Kazunari Ohgaki "Enhancement of Hydrogen Storage Rate in Pre-treated Semi-clathrate Hydrates.", *7th International Conference on Gas Hydrates (ICGH7)*, Edinburgh, July (2011).